Volume 15
Number 11
21 March 2024
Pages 3771–4188

Chemical Science

rsc.li/chemical-science

ISSN 2041-6539

ROYAL SOCIETY OF CHEMISTRY

REVIEW ARTICLE
Na Wang, Hongxun Hao *et al.*
Non-destructive real-time monitoring and investigation of the self-assembly process using fluorescent probes

Chemical Science

ROYAL SOCIETY OF CHEMISTRY

REVIEW

View Article Online
View Journal | View Issue

Cite this: *Chem. Sci.*, 2024, **15**, 3800

Non-destructive real-time monitoring and investigation of the self-assembly process using fluorescent probes

Xiongtao Ji,[a] Na Wang,*[abc] Jingkang Wang,[abc] Ting Wang,[abc] Xin Huang[abc] and Hongxun Hao*[abc]

Self-assembly has been considered as a strategy to construct superstructures with specific functions, which has been widely used in many different fields, such as bionics, catalysis, and pharmacology. A detailed and in-depth analysis of the self-assembly mechanism is beneficial for directionally and accurately regulating the self-assembly process of substances. Fluorescent probes exhibit unique advantages of sensitivity, non-destructiveness, and real-time self-assembly tracking, compared with traditional methods. In this work, the design principle of fluorescent probes with different functions and their applications for the detection of thermodynamic and kinetic parameters during the self-assembly process were systematically reviewed. Their efficiency, limitations and advantages are also discussed. Furthermore, the promising perspectives of fluorescent probes for investigating the self-assembly process are also discussed and suggested.

Received 5th December 2023
Accepted 22nd January 2024

DOI: 10.1039/d3sc06527h

rsc.li/chemical-science

1. Introduction

Self-assembly is a process in which building blocks are autonomously driven into supramolecular structures[1,2] and is a powerful tool for constructing supramolecular materials for many applications, ranging from energy harvesting to biomedicine.[3,4] These building blocks may be the same or different, and the interactions (noncovalent type) between these blocks evolve from a less ordered state (such as solutions, disordered aggregates or random coils) to a final ordered state (such as crystals or supramolecular fibers). Supramolecular structures that emerge through self-assembly are generally triggered by changing environmental variables, which create a driving force that pushes the system to a final thermodynamic minimum.[5]

[a]*National Engineering Research Center of Industrial Crystallization Technology, School of Chemical Engineering and Technology, Tianjin University, Tianjin 300072, China*

[b]*Collaborative Innovation Center of Chemical Science and Engineering (Tianjin), Tianjin 300072, China*

[c]*State Key Laboratory of Chemical Engineering, School of Chemical Engineering and Technology, Tianjin University, Tianjin 300072, China. E-mail: wangna224@tju.edu.cn; hongxunhao@tju.edu.cn; Fax: +86-22-27374971; Tel: +86-22-27405754*

Xiongtao Ji

Xiongtao Ji is studying his PhD in Chemical engineering from National Engineering Research Center of Industrial Crystallization Technology, School of Chemical Engineering and Technology, Tianjin University, under the supervision of Prof. Jingkang Wang and Prof. Hongxun Hao. His research interest focuses on the fluorescent probe design and supramolecular self-assembly for multifunctional gels.

Na Wang

Na Wang received his PhD National Engineering Research Center of Industrial Crystallization Technology, School of Chemical Engineering and Technology, Tianjin University, under the supervision of Prof. Hongxun Hao in 2020. Then, she joined the National Engineering Research Center of Industrial Crystallization Technology as an assistant professor fellow. Her research interests focus on the molecular self-assembly and design of supramolecular synthon.

Recently, the self-assembly theory and its applications have rapidly developed.[6–8] In nature, chemicals can be ubiquitously self-assembled into hierarchical and highly functional structures in a regular manner.[5,9] The building blocks of small molecules composed of the elements of the same types, such as bases, amino acids and glucose, can self-assemble into biological macromolecules, such as DNA, RNA, proteins and polysaccharides. In addition, biomacromolecules can be further assembled into cell membranes, ribosomes and chromosomes, with different functions and roles. Finally, an organelle with a spatial structure and function formed by the self-assembly of these higher structures constitute biologically active cells.[10–12] Therefore, understanding the assembly of building blocks into functionalized cell tissues is one of the fundamental topics and subjects in biology.[13] Nevertheless, owing to the complexity of the environment and aggregate structures, a non-invasive and efficient detection method is urgently needed.

Inspired by the phenomenon of *in vivo* self-assembly, researchers have designed and prepared advanced materials with desired functions through the directional control of hierarchical self-assembly *in vitro*, aiming to realize a controllable self-assembly system and its functionalization.[14–18] By designing and synthesizing building blocks with specific functional groups and specific bonding arrangements, locally ordered aggregates can be self-assembled *via* non-covalent interactions between building blocks. Additionally, in the higher-level self-assembly process, locally ordered aggregates can be further designed and assembled into materials with specific functions by controlling the external environment of the subsequent self-assembly, such as temperature and pH, and/or by regulating the interactions between aggregates or dynamics matching depending on the special morphology.[19,20] In summary, the whole self-assembly process is expected to achieve precise precoding and traceability, ensuring that the designed functions would be transferred or even magnified from the molecular level to the nanoscale or micrometer level.

The self-assembly of chemical entities is a very attractive way to create various ordered functional structures and complex substances.[21] Also, isolating the role of building blocks for self-assembly provides insight into the ordering of molecules and the crystallization of colloids, nanoparticles, proteins, and viruses.[22] Great efforts have been devoted to the preparation of

Jingkang Wang

Jingkang Wang received her PhD from Tianjin University. In 1999, she was elected an academician of the Chinese Academy of Engineering. She works as a Professor at Tianjin University, Tianjin, China. She has served as the deputy director of the Chemical and Chemical Teaching Steering Committee of the Ministry of Education, the director of the Chemical Engineering sub-committee, the chairman of Tianjin Science and Technology Association, and the vice chairman of the Municipal Overseas Chinese Federation.

Xin Huang

Xin Huang, PhD, is an assistant professor at the School of Chemical Engineering and Technology, Tianjin University. He is a member of Yongjiang Talent Innovation Team. His research interests focus on basic theoretical research in the field of industrial crystallization and supramolecular chemistry.

Ting Wang

Ting Wang received his PhD National Engineering Research Center of Industrial Crystallization Technology, School of Chemical Engineering and Technology, Tianjin University, under the supervision of Prof. Jingkang Wang in 2019. Then, he joined the National Engineering Research Center of Industrial Crystallization Technology as an assistant professor fellow. His research interests focus on optical function materials like fluorescent probes, phosphorescent materials and photoresponsive crystals.

Hongxun Hao

Hongxun Hao, PhD, is Distinguished Professor at the School of Chemical Engineering and Technology, Tianjin University. Dr Hao's research has been focused on industrial crystallization, optical function materials and supramolecular chemistry. He has authored or coauthored more than 300 papers. In addition, he has about 50 patents granted. His research achievements winning 2 national science and technology awards and a number of provincial and ministerial awards.

supramolecular structures based on different chemical building blocks. However, a comprehensive understanding of the mechanisms and the ability to monitor and control the assembly processes are critical.[21] One of the most critical issues is how to comprehensively characterize and monitor the self-assembly process,[23–25] which includes not only the evolution of morphology but also the properties of aggregates, such as the conformation of building block arrangement, surface potential, and number and concentration of aggregates. Through omnibearing detection, a more comprehensive understanding about the self-assembly process of substances could be achieved, thereby helping to accurately control the shape and properties of aggregates.[26,27]

Another significant issue in exploring the self-assembly process and mechanism of aggregates is to reveal the kinetic or dynamic evolution pathway. Currently, most researches focus on the structural evolution of aggregates, although several systematic researches on the dynamic processes have been carried out.[28,29] The main obstacle to its further development is the lack of effective methods to track the initiation and continuation of the assembly as well as to achieve the precise detection and characterization of micro-environmental parameters during the self-assembly process.[7] Generally, parameters such as temperature and pH are important and may affect the occurrence, duration and termination of the self-assembly process from the beginning to the ending.[30–32] Furthermore, the self-assembly process can occur simultaneously in the subnanoscale (molecules and ions), the nanometer to micron scale (supramolecular clusters and colloidal particle), and some higher functional structural systems. Therefore, higher requirements are put forward on the detection of micro-environmental variables, especially on the complex assembly processes in organisms.

The fluorescent probes, also known as fluorescent chemosensors, are a class of fluorescent molecules with characteristic luminescence in the ultraviolet-visible-infrared region, and the fluorescence properties can change sensitively with the change in the microenvironment.[33] The continuous monitoring of analytes can be achieved utilizing the changes in the fluorescence signals.[34] When excited by the excitation light of a specific wavelength, the electron absorption energy of the fluorescent molecule will transit to the excited state, and then the electrons might move from the excited singlet state to the ground state through radiation. During the 'move' process, the electrons release the excess energy in the form of luminescence, thus generating fluorescence.[33] Whether a molecule can produce fluorescence is mainly affected by its own structure and external environment. Generally, the conjugated structure and electron donating groups are beneficial for enhancing the fluorescence intensity. Meanwhile, small changes in the external environment, such as polarity, pH, temperature and viscosity, can also significantly affect the excitation and emission wavelength, fluorescence intensity, and fluorescence lifetime of the probes. Therefore, simple photophysical and photochemical characteristic can be used to realize the timely response and detection of complex self-assembly processes as well as the mechanisms and microenvironment changes.[35,36] In addition, the sensitivity and designability of fluorescent probes endow it advantages in *in vivo* sampling and self-assembly process at various times and space.[37–39]

Over the past several decades, more fluorescent probes have been designed and developed for practical applications in environmental monitoring, food analysis, biochemical analysis, drug detection, disease diagnosis, and bioimaging.[40,41] Some results regarding the detailed application of carbon dots-based (CD-based) fluorescent probes for the detection of metal ions along with some sensing mechanistic insight have been reported.[42,43] Li *et al.* summarized the design strategies and sensing mechanisms of CD-based fluorescent probes and discussed their applications in the sensitive and selective detection of public safety substances, organic amines, phenols, bioactive molecules, biological enzymes, and inorganic salts.[44] Chen *et al.* highlighted the recent progress on the fluorescent probes of pH and alkali metal ions from the structure of fluorophores and introduced the sensing principle for proton and alkali metal ions in detail.[45] In particular, the studies on self-assembly have gradually shifted from mechanism observation *in vivo* to controllable directional self-assembly *in vitro*. Also, the fluorescent probes for detecting the complex environment *in vivo* will also play an important role in supramolecular self-assembly *in vitro*. However, few reviews have focused on the detection and characterization from the building block to the aggregate with fluorescence probes.

Under this background, this review will focus on the application of fluorescent probes in the detection and characterization of self-assembly process to reveal the properties of aggregates and the effect of parameters of the micro-environment. Furthermore, the prospects and development directions of fluorescent probes in the self-assembly process of substances will also be discussed.

2. Fluorescent probe

2.1 Mechanism of fluorescent probe

Generally, fluorescent probe molecules have the lowest singlet electron excitation state and large π–π conjugated and rigid planar structure and can emit fluorescence under ultraviolet or visible light excitation.[46] Several typical mechanisms of fluorescent probe are shown in Fig. 1. The probes can output and exhibit the information (like aggregate properties and micro-environment parameters) during the self-assembly process *via* fluorescence signals (like excitation and emission wavelength, fluorescence intensity, and lifetime).[41,47] Also, these fluorescence signals are generally displayed through one or more sensing mechanisms, including photoinduced electron transfer (PET), twisted intramolecular charge transfer (TICT), excited state intramolecular proton transfer (ESIPT), vibration-induced emission (VIE), or involve dual/triple sensing mechanisms.[48–50] For instance, intramolecular or internal charge transfer (ICT) is a common detection approach of probes. ICT probes typically consist of three conjugated parts: the electron donor, the electron acceptor and π-conjugated linker.[51] Due to bond substitution, cleavage, or substrate coordination, the electron density of ICT probes in the recognition group is altered after

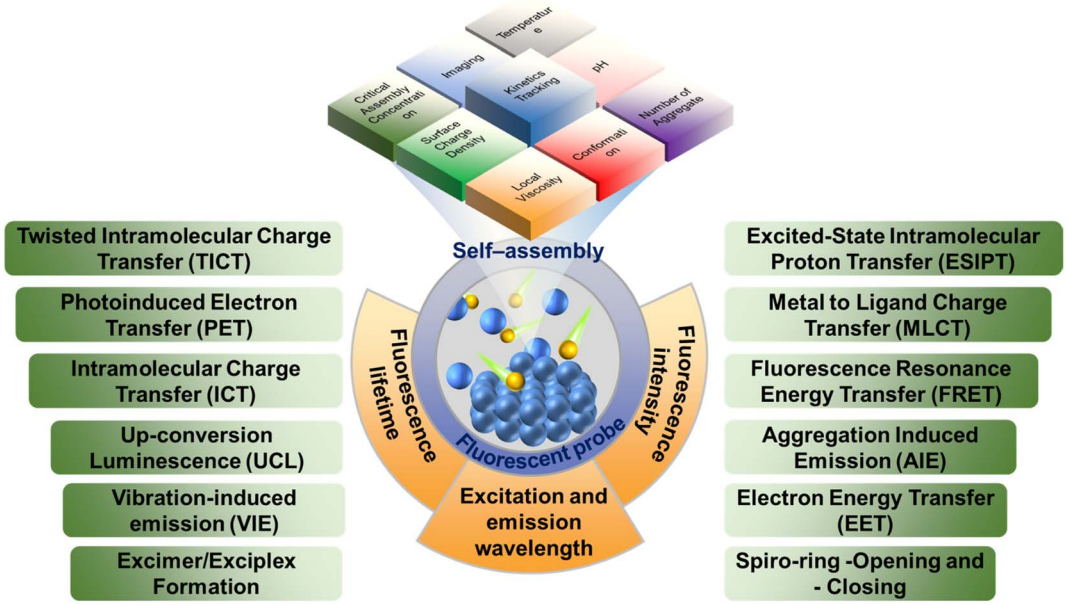

Fig. 1 Typical mechanisms of the fluorescence probe and its response to the self-assembly system.

interaction with the analyte, which would install a 'push–pull' system in the molecule. In tandem with altering the electron distribution, the excitation of the resultant species affords a large dipole and alters the excited state to that of the initial probe. Therefore, ICT probes normally present a 'turn-on' response and wavelength shift of fluorescence after interacting with the analytes. Moreover, ICT probes can also be used for ratiometric analysis in some assembly systems.[52]

For building blocks with fluorophores, the intrinsic fluorescence characteristics can be used to analyze their self-assembly process. For instance, Jelley *et al.* reported the absorption spectrum of 1,1′-diethyl-2,2′-cyanogen chloride (PIC chloride)[53,54] and found that PIC presented the J-aggregates with the side-by-side structure in water and H-aggregates with face-to-face structure in ethanol so that the spectrum of PIC chloride in aqueous solution showed significant peak narrowing and redshift, with the fluorescence enhanced compared to ethanol. Additionally, with the concentration of PIC chloride or the increase in added sodium chloride, the phenomenon was more obvious, further confirming the self-assembly and aggregates of PIC molecules.

Nonetheless, most self-assembly systems have weaker endogenous fluorescence or even no fluorophores. Hence, it is necessary to add a small amount of probe molecules to the system to detect the self-assembly by characterizing the fluorescence changes of probes. Generally, based on the steady or transient luminescence properties and quenching of probes in the self-assembly systems, the compactness of building block arrangement, phase transition, size and morphological transition of aggregates can be obtained.[55,56]

2.2 Design principle of fluorescent probe

Fluorescent probes, the sensing device that can express the chemical information of the assemblies as fluorescence signals, are typically composed of three parts:[57,58] (i) the receptors (reaction/labeling unit) that can selectively bind to the analytes and thereby change the chemical environment of probes located. The binding is generally achieved by non-covalent interactions such as coordination and hydrogen bonding. (ii) The fluorophores (signal response unit) that convert the identification signals generated by the chemical environment changes into the fluorescent signals (enhancement or decrease of fluorescence, movement of spectrum, change of fluorescence lifetime, *etc.*) to achieve the detection of the target analyte. (iii) The spacers or bridging bonds that link the receptors and fluorophores. The spacers are important factors for signal output. However, the functions of the three groups are not immutable and they can sometimes play multiple roles simultaneously.

Generally, the fluorescent probes can be roughly divided into binding fluorescent probes, displacement fluorescent probes and stoichiometric fluorescent probes. The most widely used is the binding fluorescent probes, and the comparison of fluorescence intensity, the shift of spectral positions and/or the change of fluorescence lifetimes can all serve as the references for whether the aggregations are formed during the self-assembly.[59–62] There are several factors that need to be carefully considered for the binding probe design. First of all, the probes should have high fluorescence quantum yield for the detection of complex environment, which is beneficial for improving the sensitivity of the probe. If necessary, the probes with large Stokes shifts are needed to eliminate the self-quenching of conventional fluorescent compounds. Moreover, the probes with long-wave emission can avoid the interference from background fluorescence, reduce the occurrence of fluorescence bleaching, and extend the probe lifetime. Secondly, the changes in the chemical environment during the assembly process should be fully considered so that these changes can prompt the bonding recognition between receptors and

analytes generated by acid–base reaction, coordination, or supramolecular interaction. Finally, the spacers should not interfere with the signal transmission of the probes. The detection of displacement probes is achieved by comparing the binding ability of the receptor with fluorescent indicator and the analyte.[63–65] Therefore, there are high requirements for receptors and fluorescent indicators. The fluorescent indicator needs to bind to the receptors, and the binding ability cannot be too strong. Meanwhile, the receptors should also be able to specifically identify and recognize the analytes. The probes that utilize irreversible chemical events associated with host–guest recognition have been employed as chemodosimeters for the ratiometric determination of analyte concentrations. The design principle of stoichiometric fluorescent probes with specificity and irreversibility is to address the insensitive response toward analytes.[66,67]

3 Monitoring and investigation of self-assembly

The systematic analyses of self-assembly process and aggregate properties are crucial for the design and synthesis of novel functional materials. It is even more necessary to explore the aggregates with micro-nano structure at the molecular level. Coincidentally, fluorescent probes show great advantages in the visualization of self-assembly aggregates, representation of critical aggregation state, and properties of aggregates.

3.1 Visualization of self-assembly

Recently, fluorescence probes have become a powerful tool for investigating the self-assembly process with continuous development in diagnosis and imaging[68–70] due to its advantages such as dynamic observation of assembly processes and nanoscale substructures, non-invasive image acquisition, and most importantly, specificity based on molecular sensitivity.[71] For instance, crystallization is a highly ordered self-assembly process, but it is a long-standing challenge to clearly understand the solid-state amorphous-to-crystalline transformation. The *in situ* imaging of crystal assembly relies heavily on extremely high-tech instrumentation. Ye *et al.* developed a real-time and *in situ* imaging program to record the assembly process from amorphous to crystalline.[72] The tetrasubstituted ethylene, 1,2-bis(7-bromo-9,9-dibutyl-fluorenyl)-1,2-diphenylethene (BBFT), was used. The crystal of BBFT displays dark blue emission and the amorphous form displays greenish yellow emission, with an emission difference of about 60 nm (Fig. 2a). Therefore, the phase interface between the crystalline and amorphous forms was distinguished by the fluorescence color, which is a simple and practical method

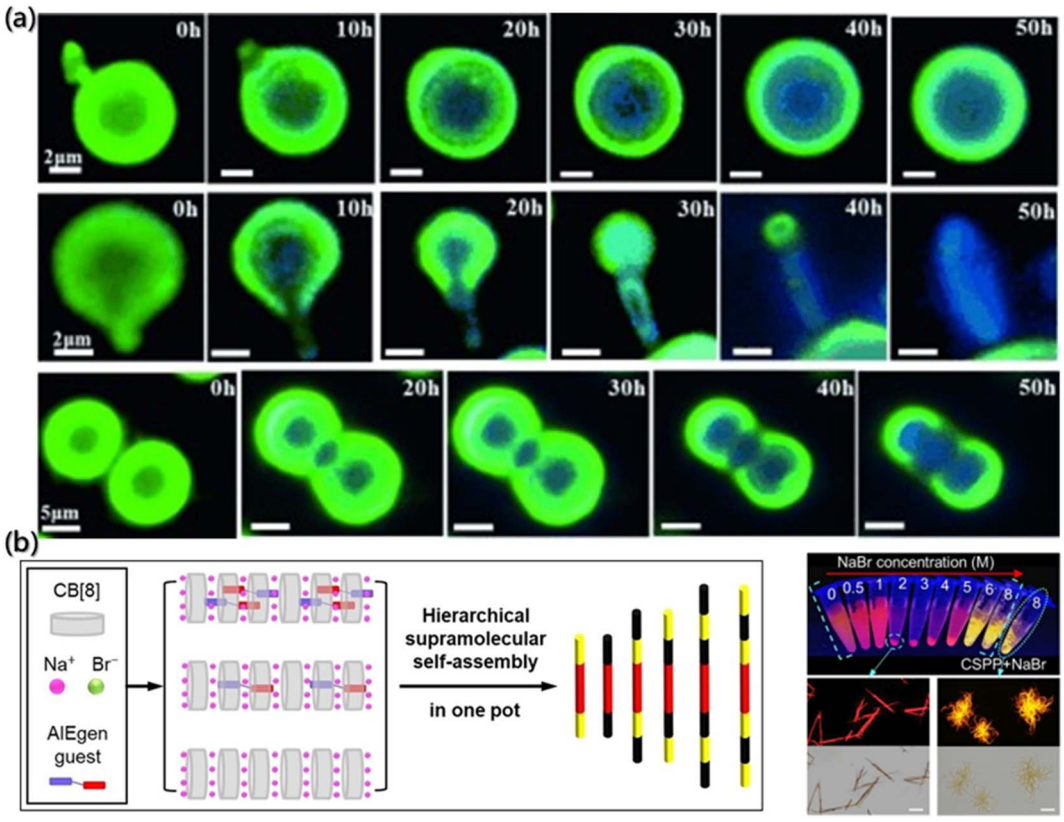

Fig. 2 (a) Fluorescence images of the assembly process of the crystal due to contact between the microparticles.[72] Reproduced with permission from ref. 72. Copyright 2015, John Wiley and Sons. (b) Fabrication of fluorescent multiblock microcolumns. (c) Imaging of the samples with different NaBr concentrations under UV light. The bottom images represent the aggregates of arrow-pointed samples at fluorescence and bright field.[73] Reproduced with permission from ref. 73. Copyright 2022, John Wiley and Sons.

to detect the internal molecular assembly of particles. The details of the important amorphous to crystalline transition were determined by fluorescence microscopy. The assembly of crystal form amorphous particles is shown at the center. However, the growth was confined to the interior of perfectly spherical particles, ending with the core–shell structure. Defects on the surface before the assembly of the crystal would lead to a complete transformation from the amorphous sphere to a ribbon-like crystal.

The visualizations of the aggregate by the fluorescent probe are not only for intuitive morphology analysis but also for the deeper exploration of the assembly mechanism. Shi *et al.* reported fluorescent multi-segment microrods formed by the complexation of cucurbit[8]uril (CB[8]) and the AIEgen guest molecules, mono((*Z*)-(4-(4-(2-cyano-2-(4-(1-methylpyridin-1-ium-4-yl)phenyl)vinyl)phenyl)-1-methylpiperazin-1-ium-1-yl)methanide) diiodide (CSPP). Also, the CB[8] can also have weak interaction with Na^+ and Br^- (Fig. 2b).[73] Based on the properties, the mechanism of multistage supramolecular self-assembly was clearly revealed by the fluorescence spectra, UV-visible absorption spectra, fluorescence lifetime and fluorescence imaging analysis. During the volatilization of the solution, NaBr was concentrated and the assembly was triggered. In Fig. 2c, the fluorescence imaging under UV light showed that the NaBr solution with the concentration of 2–5 M emitted red fluorescence. However, orange-yellow precipitates, which were located in the emission band of the CSPP monomer assembly and presented coil-like structure, were formed at NaBr concentration higher than 6 M. The metal cations would compete with the CSPP and complex with cucurbituril under the circumstances, thereby destroying the complexation of CSPP and CB[8] with the high Na^+ concentrations.

Another important aspect of fluorescent probes is monitoring the assembly of very complex natural mixtures of chemically similar molecules.[74–76] The traditional detection methods for the aggregation process extremely depend on the combination of multiple methods, such as small-angle X-ray scattering, dynamic light scattering, and atomic force microscopy. However, each method has its limitations.[77,78] Fluorescence provides a new direction for detecting the aggregation processes of complex natural mixtures. Actually, currently, fluorescence is practically the only method to study the aggregation. For instance, due to the complex interacting patterns, quantifying the formation of molecular complexes between thousands of polycyclic aromatic hydrocarbons (PAHs) mixtures is challenging. Pančе Naumov *et al.* demonstrated the potential of fluorescence for the quantification of molecular processes that are at the core of the asphaltenes' aggregation.[74] Generally, asphaltene molecules with polyaromatic cores emit light in the visible region upon excitation. However, when the small electron-deficient aromatic additives, especially surfactant-like additives with electron-withdrawing functional groups, were brought in the asphaltene mixtures, these additives would interact strongly with certain PAHs and lead to the formation of molecular complexes, resulting in the emission quenching of asphaltenes, while the excited-state lifetimes of the unbound asphaltenes remain unchanged. Therefore, it can be used for the detection of the assembly of very complex natural mixtures of chemically similar molecules.

3.2 Critical assembly concentration

The critical assembly concentration is an important parameter that must be considered for self-assembly design. Building blocks will self-assemble above the critical assembly concentration, while conversely, the aggregates will dissociate below the critical assembly concentration. For example, the surfactant molecules would enrich and adsorb into a monolayer structure at the interface. When the surface adsorption reaches the critical micelle concentration, there will be no more enrichment of surfactant molecules on the surface.[79,80] However, the interaction between hydrophobic groups still allows the molecules to escape from the water environment, and the surfactant molecules will self-aggregate in the solution. In this process, the hydrophobic groups aggregate as the core and the hydrophilic groups contact with water to form the shell.[81,82] The traditional methods for determining critical assembly concentration include surface tension method, electrical conductivity method, dye-assisted method, turbidimetry method, and light scattering method. However, these methods all have certain limitations: the surface tension method is affected by the building block concentration and inorganic salts, and electrical conductivity method is only applicable to the ionic self-assembly. Fortunately, the emission spectra of fluorescent probes are very sensitive to the changes in the micro-environment and show good prospects and advantages in determining the critical assembly concentration.[83,84]

Pyrene is a commonly used fluorescent probe molecule to determine the critical assembly concentration. Also, the peak intensity ratio (I_1/I_3) of its fluorescence at the first and third vibrational bands varies with the concentration of the amphiphilic building block in solution, and the mutation point is the critical assembly concentration.[84] Bharmoria *et al.* determined the critical aggregation concentrations of cetyltrimethylammonium bromide (CTAB) in salt solutions using steady-state fluorescence spectra of pyrene (Fig. 3a and b)[85] and found that the lower I_1/I_3 ratio indicated the relatively hydrophobic or non-polar environment due to the formation of the self-assembly structure, and the critical assembly concentration was obtained according to the mutation point on the variation curve of I_1/I_3.

Moreover, Zhu *et al.* designed a sensitive and visible fluorescence turn-on probe for determining the critical assembly concentration of ionic surfactants, based on strong aggregation-induced emission in the solution of racemic tetrahydropyrimidine (THP-1).[86] Although there is poor linear relationship between the fluorescence intensity of pure THP-1 and the concentration of ionic surfactants, a surfactant concentration detection system with good linear correlation was prepared by diluting the concentrated solution of surfactant containing THP-1. Furthermore, compared with pyrene, THP-1 is a visible and sensitive fluorescence probe with higher sensitivity, and hence it can detect the critical assembly concentration *via* the visible fluorescence turn-on mode under UV light. The critical assembly concentration values can be determined *via* the upper inflexion with the strongest fluorescence intensity of THP-1 (Fig. 3c and d), rather than the lower inflexion with the weakest fluorescence intensity. Additionally, THP-1 has robust

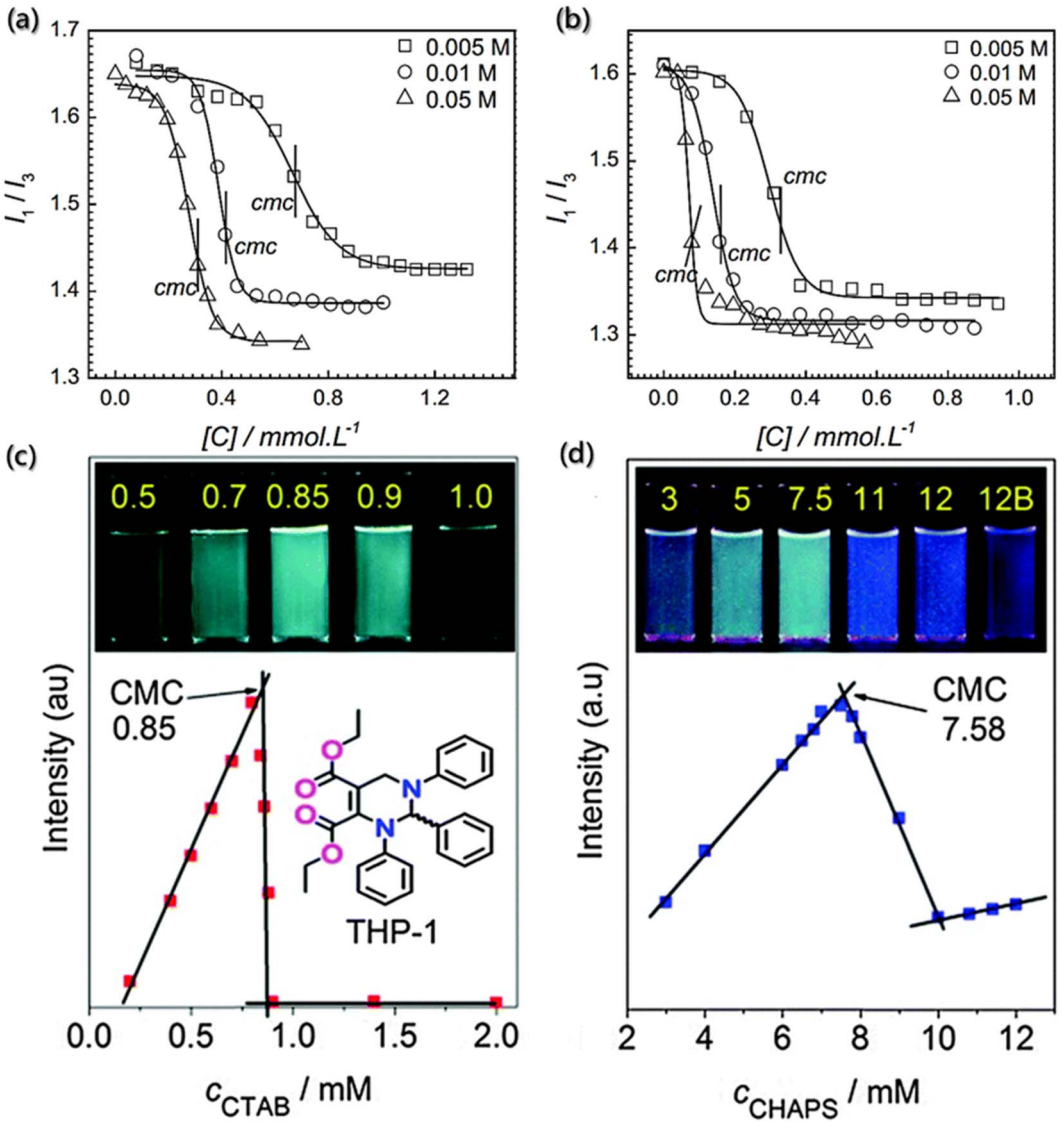

Fig. 3 Determination of critical assembly concentration using fluorescence probes. (a and b) Variation in I_1/I_3 of the pyrene probe as a function of CTAB concentration in different electrolyte concentration solutions of sodium butyrate and sodium benzoate.[85] Reproduced with permission from ref. 85. Copyright 2015, Nature Publishing Group. (c and d) Variation in fluorescence intensities at 484 nm of THP-1 as a function of the concentrations of CTAB and CHAPS (3-[(3-cholamidopropyl) dimethylammonio]-1-propanesulfonate), respectively. Insets show the samples with different concentrations of CTAB and CHAPS under UV light (365 nm).[86] Reproduced with permission from ref. 86. Copyright 2014, the Royal Society of Chemistry.

adaptability and can be used to quickly detect changes at different concentrations.

However, the design and development of probes for determining the ultra-low critical assembly concentration (such as near millimole level) or non-surfactant assembly remains a challenge.

3.3 Number of aggregates

The number of aggregates can be determined by the quenching of the fluorescence probe. In the solution with ordered molecular assembly, quenching only occurs in the aggregates containing both probes and quenchants.[87,88] Therefore, the average number of quenchers in each aggregate is expressed as the concentration ratio of the quenchants in aggregates to the total targets.

J. A. Molina-Bolívar *et al.* determined the average aggregation number of *N*-decanoyl-*N*-methylglucamide (MEGA-10) in pure water or NaCl solutions with different salt concentrations using the steady-state fluorescence quenching method.[89] In the process, pyrene and cetylpyridinium chloride (CPyC) molecules were used as the probe and the quenchant, respectively, and the fluorescence intensities of the excitation wavelength (335 nm) and emission wavelength (383 nm) were recorded. Additionally, when the concentration of the quenchant used to quench the luminescent probe is known, the average aggregation number can be obtained by the following formula:

$$\ln I_0/I = [\mathrm{Q}]N_{agg}/([\mathrm{S}] - \mathrm{cmc}) \quad (1)$$

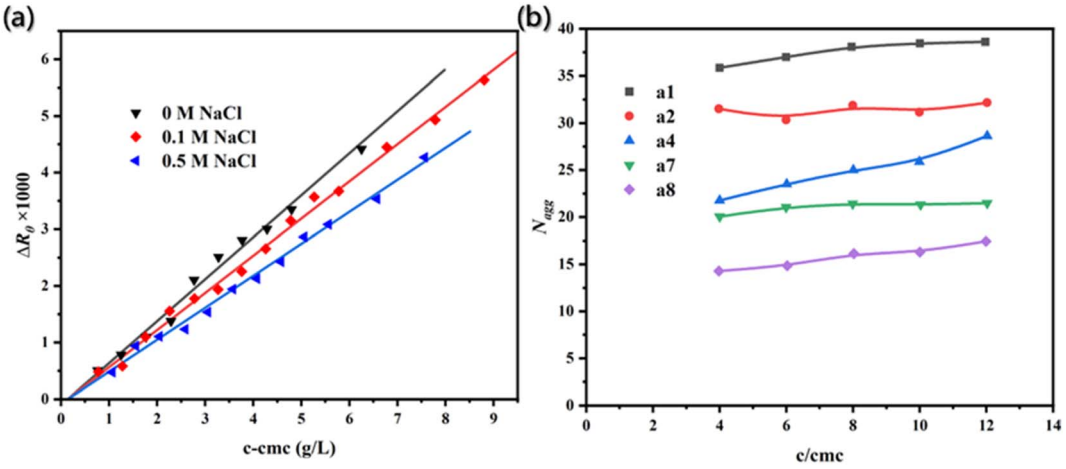

Fig. 4 (a) Excess scattering ratios (ΔR_θ) is the function of micellar concentration.[89] Reproduced with permission from ref. 89. Copyright 2007, Elsevier. (b) Aggregation number (N_{agg}) as a function of concentration c/cmc with different carbon atomic number (s) spacing between two dodecyl chains and a diamide spacer.[90] Reproduced with permission from ref. 90. Copyright 1999, American Chemical Society.

where I_0 and I represent the fluorescence intensities without or with the quenchant, respectively. N_{agg} represents the average aggregation number; cmc represents critical micelle concentration; [S] represents the total target concentration, and [Q] represents the quenchant concentration. Also, N_{agg} can be determined by the slope of $\ln(I_0/I) - [Q]$.

The static light scattering, a mature method for determining the average aggregation number, was used to evaluate the results. The molecular weight of aggregates was estimated through the linear regression of excess scattering ratio to micellar concentration (c − cmc) (Fig. 4a), and the average aggregation number was determined. The results obtained by the two different methods were found to be consistent.

Additionally, time-resolved fluorescence quenching (TRFQ) is also an important tool for obtaining the accurate aggregation number by measuring the fluorescence attenuation curve of probes and then fitting the data with appropriate kinetic models. Notably, TRFQ can realize the direct measurement of aggregation number.[90]

For instance, Pisárik *et al.* determined the assembly aggregation numbers of cationic bisammonium gemini surfactants (a(s) and e(s)) using pyrene as the fluorescent probe and cetylpyridinium chloride as the quenchant, respectively.[91] The concentration ratio of aggregates to quenchants was set close to 1 to ensure that each aggregate contained one quenching molecule. Generally, the fluorescence attenuation of each aggregate containing different number of quenched molecules is usually non-exponential, according to the TRFQ kinetic model. However, due to the Poisson distributed quenchants on the aggregates, the attenuation curve of pyrene is a single index. Also, the attenuation curve is obtained by the following formula

$$I(t) = I(0)\exp\{-t/\tau_0 - R[1 - \exp(-t/\tau_Q)]\} \quad (2)$$

where $I(t)$ and $I(0)$ represent the fluorescence intensities at time t and time 0, respectively. τ_0 and τ_Q represent the fluorescence lifetime of probes without and with the quenchant; R, the fitting parameter, represents the concentration ratio of quenchant (c_Q) to the aggerates (c_{mic}).

Therefore, the fluorescence attenuation curves at excitation wavelength (340 nm) and emission wavelength (381 nm) were both recorded, and then the aggregation number (Fig. 4b) of surfactants with different carbon atomic number spacing between two dodecyl chains and a diamide spacer could be calculated by the following formula.

$$N_{agg} = (c - \text{cmc})/c_{mic} = R(c - \text{cmc})/c_Q \quad (3)$$

3.4 Surface charge density

The surface charge density of aggregates is the key parameter to understand the formation and subsequent behavior of aggregates, which is usually measured by the zeta potentiometer. However, accurate results are difficult to obtain by zeta potentiometer for many systems with complex components, high concentration and diverse interaction. Coincidentally, it is very gratifying that the fluorescent probes with high specificity show a very promising application prospect in the qualitative study of surface charge density.[92,93]

Characterizing the fluorescence quenching efficiency is one of the effective methods for charge density analysis. In this method, the charged quenchants need to be added to the assembly system with probe molecules, and the changes in the fluorescence intensity are detected to determine the electrical properties and charge density on the aggregate surface. Jiang *et al.* used pyrene as the fluorescence probe and established the aggregate growth model on the mixed ion surface induced by β-cyclodextrin (β-CD) (Fig. 5a).[94] The quenching efficiency of pyrene increased with the increased surface charge density of aggregates due to the quenchants (Cs^+ and $S_2O_3^{2-}$) in sodium dodecyl sulfate/dodecyltriethylammonium bromide (SDS/DEAB) solution. However, the added β-CD can selectively combine with cationic or anionic groups to form neutral aggregates approaching 1 : 1 stoichiometry of the anionic/

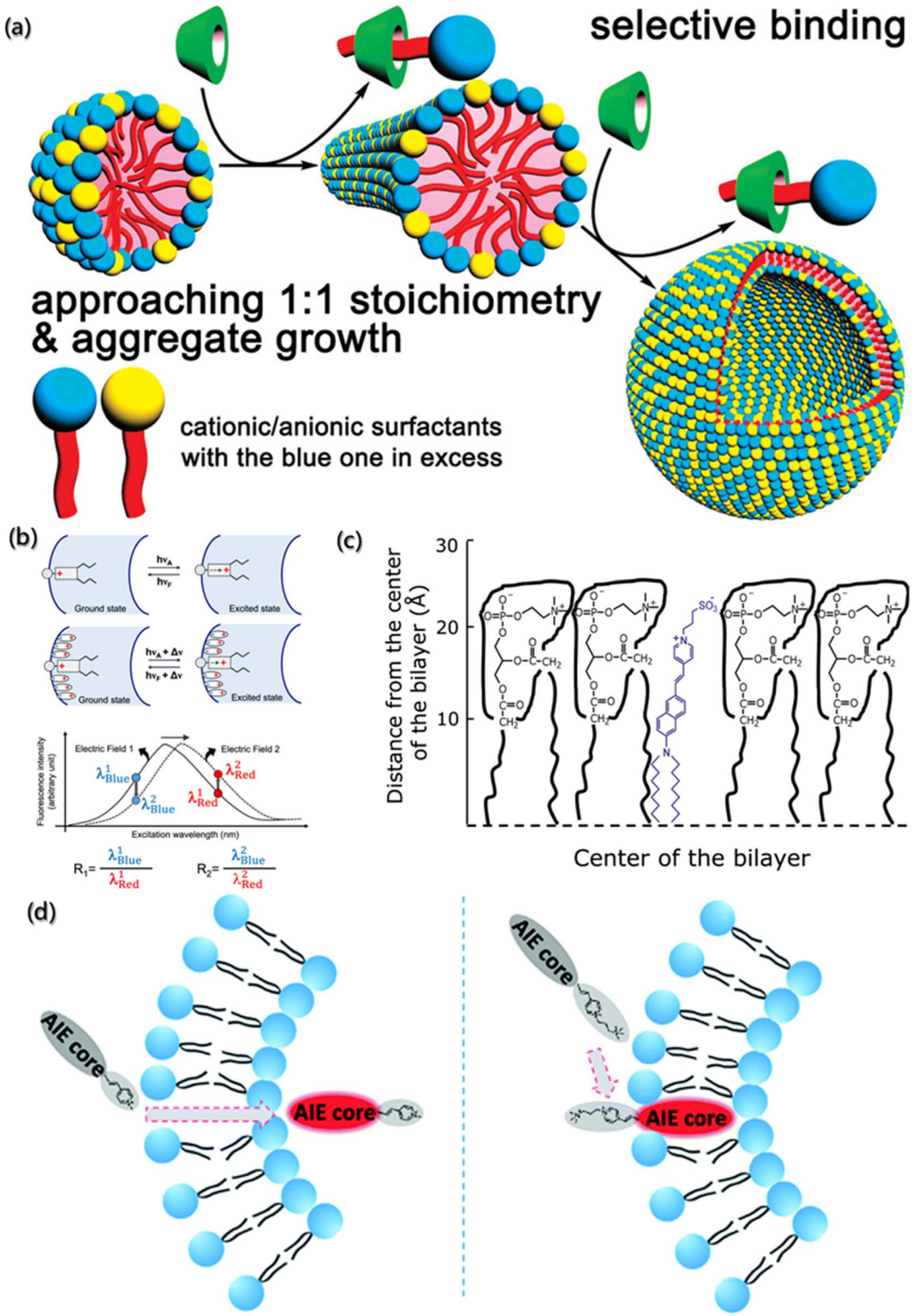

Fig. 5 (a) Aggregate growth of surfactant with cationic and anionic induced by β-CD.[94] Reproduced with permission from ref. 94. Copyright 2009, American Chemical Society. (b) Representation and fluorescence excitation spectra of electrochromic probes bound to the membrane (λ_{Blue} = blue edge of the spectrum; λ_{Red} = red edge of the spectrum; R = fluorescence intensity ratio).[95] Reproduced with permission from ref. 95. Copyright 2022, American Chemical Society. (c) Schematic representation of the localization of di-8-ANEPPS in the membranes.[96] Reproduced with permission from ref. 96. Copyright 2012, Elsevier. (d) Schematic illustration and structure of AIEgens.[97] Reproduced with permission from ref. 97. Copyright 2019, the Royal Society of Chemistry.

cationic building block and leading to a decrease in the surface potential. Therefore, the quenching efficiency decreased significantly with the addition of β-CD.

In addition, Loew has developed the voltage-sensitive fluorescent probes for the dipole potential measurement of molecular assemblies.[98] As shown in Fig. 5b, voltage-sensitivity probe is electrochromic. When probe molecule is excited from the ground state to the excited state, electronic charge will present a large movement. If the direction of charge movement is parallel to the external electric field, the transition energy would be extremely sensitive to the strength of the electric field, and the change in the dipole potential will change the energy needed to excite the chromophore. Hence, the fluorescence intensity decreases at low wavenumber and increases at high wavenumber, and the ratio of the two intensities represents a measure of the probe's response to the electric field.[95,99] For example, Haldar *et al.* designed a voltage-sensitive probe molecule of 4-(2-(6-(dioctylamino)-2-naphthalenyl)ethenyl)-1-(3-sulfopropyl)-pyridinium inner salt (di-8-ANEPPS), which is mainly characterized by the hydrophilic receptors and two hydrocarbon chains, making the fluorescent groups parallel to the lipid molecules (Fig. 5c).[96] Normally, the chromophore of naphthyl styrene in the ground state has a positive charge near the pyridine nitrogen. After excitation, the chromophore undergoes a large charge redistribution, and the positive charge moves to near the aryl amino nitrogen in the excited state. Moreover, due to the hydrophilic part and the hydrocarbon chains, the probes are easily inserted between the amphiphilic lipids of membrane. The dipole potential (φ_d) of 1-palmitoyl-2-oleoyl-*sn*-glycero-3-phosphocholine (POPC) was determined by the linear relationship ($\varphi_d = (R + 0.2)/4.3 \times 10^{-3}$) between dipole φ_d and R.

Furthermore, the voltage-sensitive probes also show exciting application prospects in biofluorescence imaging. Unlike the *in vitro* processes, the factors that need to be considered for intracellular assembly imaging probes within cells are fluorescence emission wavelength, membrane penetration, solubility, and stability. Zheng *et al.* designed and synthesized a series of selective probes for sub-organelle imaging,[97] as shown in Fig. 5d. In these voltage-sensitive probes, the hydrophobic section and pyridine groups were designed for the emission behavior, and the charged groups were designed for the permeability of the cell membrane. Further simulation calculations revealed that TPEPy and TPy with positively charged pyridine could pass through the cell membrane and "light up" the mitochondria, while TPEVP and TVP with the pyridine group and quaternary 3-(trimethylammonio) propyl group could directly "light up" the cell membrane.

3.5 Conformation

The conformation is the key and theme for self-assembly process analysis and monitoring, which directly reflects the assembly mechanism of building blocks and the possible function of aggregates.[7] Currently, the main method for conformation research is spectroscopy, including nuclear magnetic resonance (NMR), circular dichroism (CD), laser Raman, and infrared spectroscopy.[27,100] Neutron diffraction is also an important means for conformation investigation, although expensive instruments and weak support theory restrain its development.[101] In addition, some researchers have also attempted to infer the conformation of aggregates from the ordered crystal structure assembled by aggregates. However, the reverse inference from the final product is not universal and it is difficult to analyze the structure of macromolecule and its aggregates.[102,103] Fluorescence spectra can perfectly address the defects and shortcomings of the above methods, with the

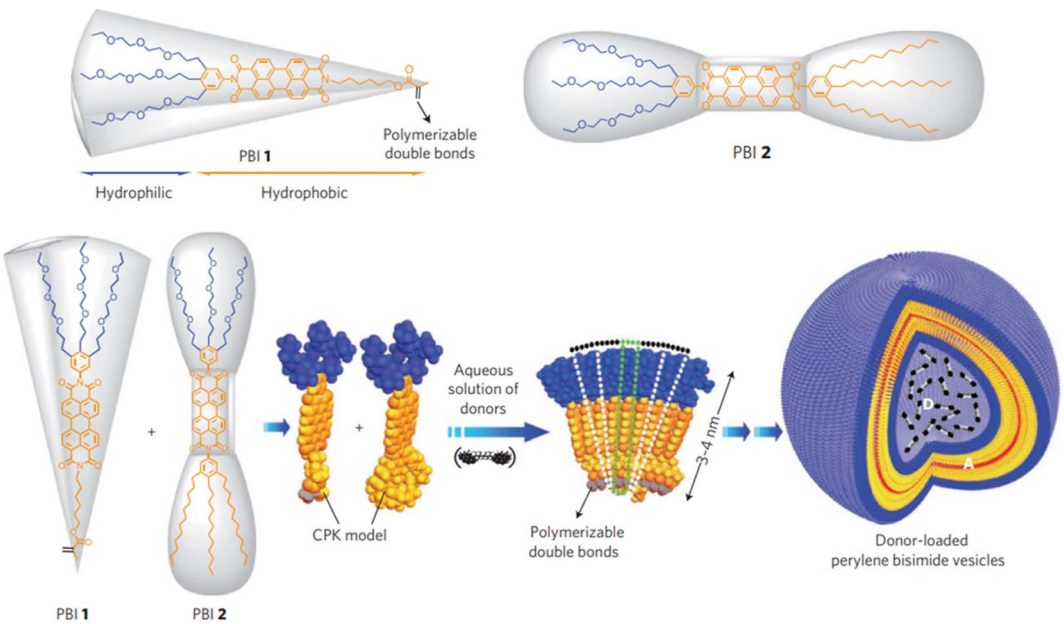

Fig. 6 Assembly of donor-loaded perylene bisimide vesicles by changes in spontaneous curvatures in water.[106] Reproduced with permission from ref. 106. Copyright 2009, Nature Publishing Group.

advantages of high sensitivity, strong selectivity, low dosage and rigorous results.[104,105]

Xin Zhang *et al.* reported the assembly of perylenebisimide with different proportions of hydrophobic and hydrophilic fragments.[106] The double layer vesicles were formed by the aggregation of wedge-shaped amphiphile with a hydrophobic hexylester chain and a hydrophilic triethylene glycol chain and were photopolymerized by the terminal double bond (Fig. 6). In the presence of acid-sensitive bis-pyrene triamine, the prepared vesicles were trapped in the aqueous cavity. Hence, the photopolymerized particles formed a stable FRET-based fluorescent pH sensor over the entire range. The open conformation of dipyrene was constrained by electrostatic forces between the protonated amines of the donor at low pH. The pyrene monomer emitted in the range of 370–420 nm at 363 nm excitation. At high pH, π–π interactions were maximized due to the closed conformation. The overlap of this stacked conformation's green emission and perylene diimide absorption promotes the energy transfer. It provides ultrasensitive pH information with fluorescent color changes covering the entire visible range.

With the development of characterization tools, high-quality mass spectrometry (MS) has been used to identify building blocks or polymers and to evaluate the heterogeneity degree. Also, the combination of FRET and MS has been proposed to detect the conformation, stability and kinetics of aggregates, which shows great advantages for aggregates analysis in gas phase.[107] As shown in Fig. 7a and b, Tiwari *et al.* designed a transition metal ion FRET (tmFRET) fluorescence probe using rhodamine 110 as the donor and Cu^{2+} as the acceptor[108] to detect the conformational changes of aggregates in the range of 10–40 Å. They found that the FRET efficiency decreased as the distance between the donor and acceptor increased and proved the inflated structure of peptide sequence in the gaseous state, accompanied by the loss of helicity (Fig. 7c).

Another ingenious and useful application of FRET is molecular beacons (MBs) for DNA conformation and structure detection[109] and further for the assembly processes in organisms. After discovering the double helix structure of DNA, Tyagi and Kramer reported for the first time about MBs, the strongest and specific base pairs, based on biomolecule recognition.[110] Generally, MBs are the DNA sequence composed of a target-

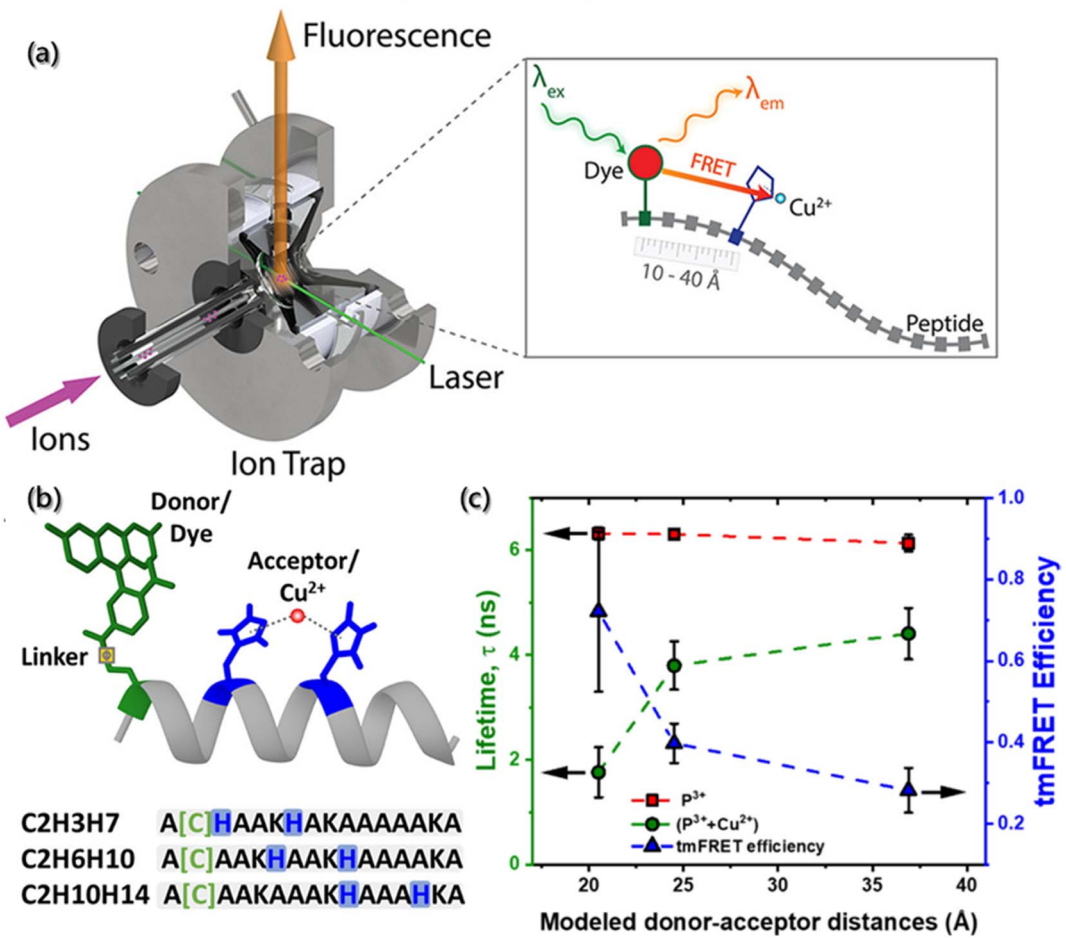

Fig. 7 (a) Experiments of selected-ion gas-phase fluorescence. With the laser beam, ions of interest are mass-selected and irradiated, then the emitter fluorescence is used for measurements. (b) Structure of helical peptides with dye-labeled cysteine and H residues complexed by Cu^{2+}. (c) Lifetimes and tmFRET efficiencies in peptides (P) and their complexes with Cu^{2+}.[108] Reproduced with permission from ref. 108. Copyright 2021, American Chemical Society.

recognition region of about 15–30 bases flanked by two short complementary stem sequences, which force the entire sequence to form a stem-loop structure in the absence of a target.[109] The MB stem-loop structure holds the fluorescence-donor and fluorescence-acceptor moieties in close proximity to one another, which results in resonant energy transfer and then fluorescence quenching. However, once the system contains target DNA or RNA, a spontaneous conformation change occurs upon hybridization to separate the two moieties and restore the fluorescence.

4. Micro-environment response

Self-assembly is an important method of material design and a spontaneous process of intermolecular interactions between building blocks formed by ions, molecules, clusters, *etc.* Typically, self-assembly is carried out at an interface and/or in solution with the special micro-environment and driven by specific temperature, pH, light, polarity, *etc.*, to allow the required motion of building blocks. The driving force causes building blocks to move into the final aggregates through the different possible configurations. Also, driven by the micro-environment, thermal motion provides a major part of the motion required to enables molecules contact each other. Therefore, there are many ways to trigger and/or drive the self-assembly by gradually changing the micro-environmental conditions (such as building block concentration, temperature, pH, ionic strength, and solvent) or using an external inputs (such as light and field-stimulation) and ultimately form a stimulus-responsive mechanism.[111]

These stimulus-responsive self-assemblies are considered as an intelligent behavior, which can accept signals from the external environment to actively change the structure of the assembly and further respond to form corresponding functionalities.[112,113] Currently, the stimulus-responsive self-assembly has been attractive in the field of nanomaterials, life science and clinical medicine.[114,115] Additionally, fluorescent probes can monitor multiple analytes/parameters of micro-environments. Inspired by this, the detection of micro-environments using fluorescent probes can help monitor the assembly process and even achieve the precise control of assembly.

4.1 Temperature

As an important parameter of the system, temperature can affect the self-assembly process and aggregate properties. The self-assembly rate and the diffusion rate of building blocks are roughly affected by temperature. In addition, the temperature distribution reflects the thermodynamics (exotherm or endotherm) of specific location of the assembly system. Generally, the measurement is realized indirectly by the changes in the performance with temperature, such as the expansion thermometer based on volume change, resistance thermometer based on electrical conductivity change, infrared thermometer based on blackbody radiation, *etc.* However, these thermometers do not have spatial resolution or sensitivity for microfluidic or micro-thermometric regions due to the heat exchange equilibrium time and disturbance time between the probes and objects.[116–118] Moreover, temperature also has a significant impact on the non-radiative transition constant of fluorescent substances, which in turn weakens or enhances the fluorescence intensity. Therefore, the fluorescence thermometers have been proposed to sense temperature fluctuations,[119] which is achieved by monitoring the changes in the fluorescence intensity or lifetime of the fluorescent probes added into the system.

Fluorescence thermometers are mainly composed of single-wavelength fluorescence intensity response and ratiometric fluorescence temperature sensing. During the change in the absorbing light from the ground state (S_0) to the lowest excited singlet state (S_1), the molecules at S_1 will be deactivated by radiative transition or non-radiative transition. Based on the response of a single excited state to temperature, single-wavelength fluorescence temperature sensors have been proposed, which could be divided into the fluorescence quenching type and fluorescence enhancement type.[120] For example, Arai *et al.* targeted the enrichment and measured the temperature of subcellular endoplasmic reticulum (ER) using the temperature-dependent fluorescence quenching probe with the temperature sensitivity of 0.039/°C at 0–5 °C.[121] By modifying the side chains of the probe skeleton, a compound (BDNCA346) was further designed for the specific recognition of ER, which was called ER thermo yellow. The fluorescence intensity of the probe decreases with increasing temperature and can be restored after cooling due to no precipitation and degradation of the probe. The temperature sensitivity of ER thermo yellow was evaluated by the microscopic system with a near infrared laser (1064 nm), and it was found that the temperature change was controlled by focusing distance and laser power (Fig. 8a). After multiple heating and cooling cycles, ER thermo yellow displayed a series of square waves as a response to temperature changes, while the commercial ER trackers do not show square waves (Fig. 8b).

However, the fluorescence of the quenching probe usually weakens with the increasing temperature, affecting the sensitivity of temperature measurement. Besides, probes with larger quenching range often have weaker fluorescence intensity at higher temperature, which is not conducive to accurate measurement within a large temperature range. Therefore, some researchers have designed enhanced fluorescence temperature sensors utilizing conformational changes caused by heating to suppress the non-radiative transition at elevated temperature.[124,125] A common method is to modify the probe molecules on polymer or DNA, regulate the deactivation of fluorescent molecules at the excited state by the temperature response, and then achieve the temperature sensing. Ebrahimi *et al.* designed such a nanometer thermometer with multi-temperature sensing ranges[122] and used gold nanoparticles (AuNPs) as the molecular beacons (MB). In order to avoid the problem of low-resolution when multiple probes measure over a wide temperature range, multiple labeled MBs are used as the sensor elements to simultaneously modify the AuNP surfaces (Fig. 8c). The melting curves confirmed that immobilizing different types of MBs on the same AuNP have no negative effect on the sensing functions. The

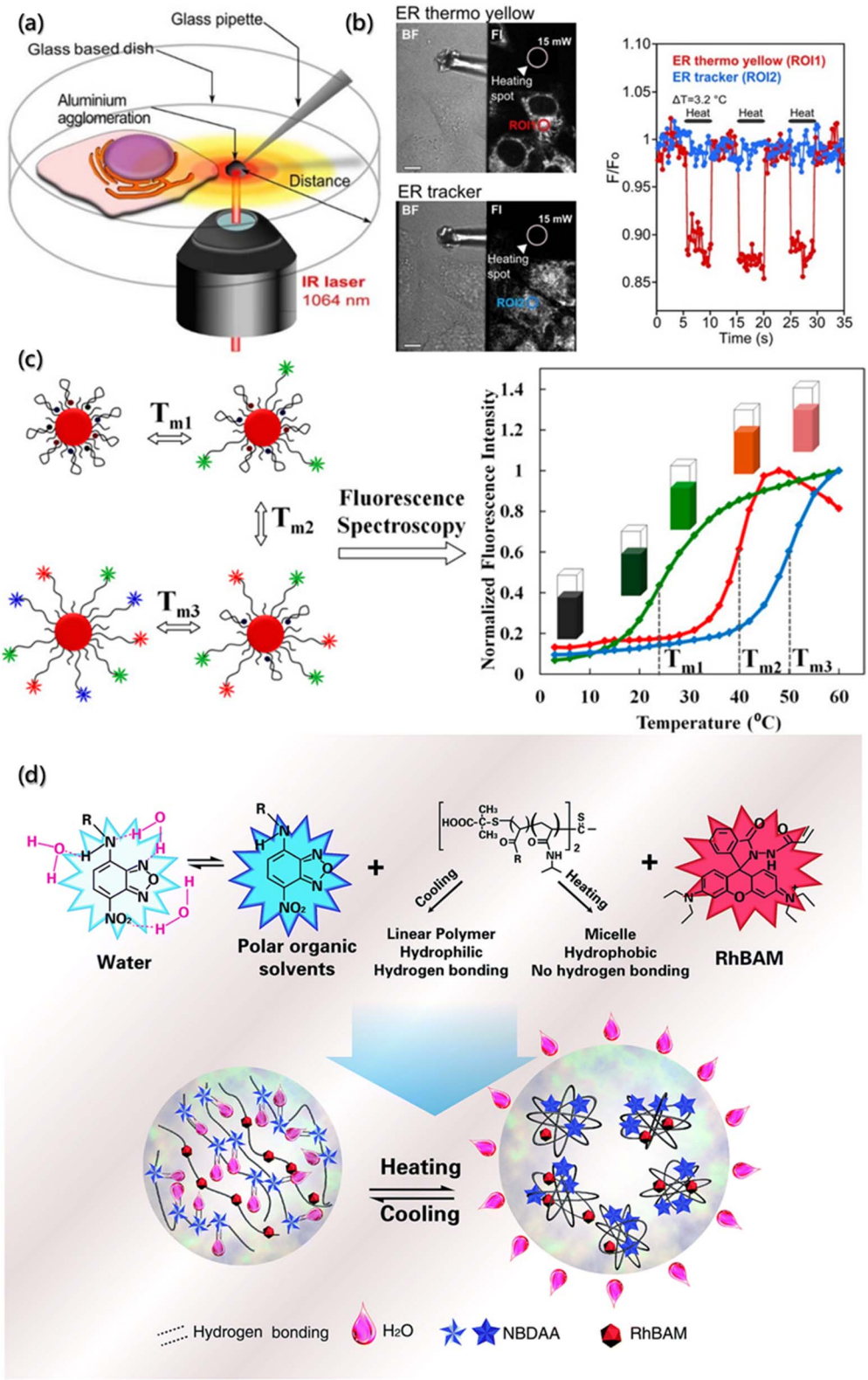

Fig. 8 Temperature determination of the micro-environment by a fluorescence probe. (a) Schematic illustration of the temperature measurement and evaluation system based on confocal laser scanning microscopy with an infrared laser. (b) The regions generated by an infrared laser and corresponding temperature sensitivity of ER thermo yellow and ER tracker. Scale bars are 10 μM.[121] Reproduced with permission from ref. 121. Copyright 2014, Nature Publishing Group. (c) Schematic illustration of nanometer thermometer with multi-temperature sensing range and corresponding melting curves.[122] Reproduced with permission from ref. 122. Copyright 2014, American Chemical Society. (d) Schematic illustration and structures of the ratiometric fluorescent polymers.[123] Reproduced with permission from ref. 123. Copyright 2014, Royal Society of Chemistry.

resolution of the nanoprobe was less than 0.50 °C in the range of 15–60 °C, making it suitable for temperature measurement at the micrometer or nanometer scale.

The single-wavelength intensity response is easily affected by the uneven distribution of samples and fluctuation of excited light intensity, resulting in low accuracy.[126] Subsequently, the ratiometric fluorescence temperature sensors system with self-calibration was proposed, which featured increased signal-to-noise ratio and thus much more reliable quantification. They harvested the fluorescence intensity changes from two or more emission bands at different wavelengths.[127] Qiao *et al.* synthesized a nanothermometer of ratiometric fluorescent polymer for intracellular temperature sensing using living/controlled reversible addition–fragmentation transfer polymerization (Fig. 8d).[123] The fluorescence thermometer consisted of a thermosensitive polymer (poly-*N*-isopropylacrylamide, PNIPAm), a polarity sensitive fluorescent dye (4-(2-acryloylaminoethylamino)-7-nitro-2,1,3-benzoxadiazole, NBDAA) and a rhodamine B derivative (RhBAM). They found that fluorescence quenching occurred at lower critical solution temperature (LCST) because the molecular segment was linear, and the NBD chromophore in the segment formed hydrogen bonding with the water molecules in the solvent. On the other hand, above the LCST, the molecular segment shrank, and NBD was separated from hydrolysis due to the increased hydrophobicity of the environment, resulting in a significant enhancement of fluorescence. The ratiometric fluorescence thermometer was further used to measure the fluorescence emission intensity excited by two different wavelengths through self-calibration to eliminate most of the ambiguities owing to the single-wavelength intensity response of the environment and thus distinguished the temperature differences less than 1.0 °C.

4.2 pH

Potential of hydrogen (pH) is one of the most relevant parameters in aqueous solutions. During the self-assembly process, the pH value not only affects the interfacial properties of aggregates but also affects the ion flow of assembly. The degree of protonation and deprotonation of building blocks with ionizable groups can be manipulated by the pH environment so that their electrostatic interactions will be controlled. Additionally, the strength of ionic interactions can also be affected due to the changes in pH and the addition of multivalent ions or other charged blocks. The most common acquisition method to obtain these data in analytical chemistry is to directly measure the potential between the two electrodes. However, the self-assembly process analysis requires *in situ* measurements without any physical interaction, and the determination of local pH offers a unique and major opportunity to increase our understanding of the self-assembly system. Due to the non-invasive optical properties, fluorescent pH-sensitive probes are a powerful tool for the determination of the local pH value.[47,128]

One of the important fluorescent pH sensitive probes is the "turn-on" probe, which can easily distinguish the "on" or "off" state when the pH is imbalanced. Chakraborty *et al.* reported a fluorescent pH-sensitive probe (PS-OH) synthesized from pentacyclic pyrylium fluorophore (PS-OMe) demethylated by boron tribromide (Fig. 9a).[129] Due to the deprotonation of phenol-OH, the mixed state electrons transited from the asymmetric highest occupied molecular orbital (HOMO) to the symmetric lowest unoccupied molecular orbital (LUMO), which indicated the non-emission properties of PS-OH at neutral and alkaline pH. Therefore, the maximum absorbance at 460 nm gradually decreased, while a new maximum absorbance appeared at 570 nm as the pH value of the system increases. On further applying the PS-OH probe to detect the changes of intracellular pH, it was found that fluorescence was not observed at pH = 7.4. When the pH value dropped to 7.0, detectable fluorescence signals were observed, and the fluorescence intensity gradually increased with the decrease of the pH value. Therefore, PS-OH is capable of monitoring even a minute change in the physiological pH in cells during the therapeutic process with chemodrugs or apoptotic agents in real time.

Compared with pH probes with single emission intensity, the ratiometric fluorescent pH sensitive probes can simultaneously detect two signals at one time, making the data more reliable and avoiding the influence of environment and concentration on the fluorescence intensity.[132] The response mechanisms of ratiometric probes are mainly based on through bond energy transfer (TBET), intramolecular charge transfer (ICT), excited-state intramolecular proton transfer (ESIPT), fluorescence resonance energy transfer (FRET), *etc.* Dennis *et al.* used semiconductor quantum dots (QD) as donors and pH-sensitive fluorescent protein (FP) as acceptors to design and synthesize FRET pairs (Fig. 9b).[130] The FRET pair takes full advantage of the excellent brightness, high quantum yield and photostability, binding capacity with multiple acceptor molecules, wide excitation spectrum, narrow and adjustable emission spectrum of QD as the donor, and the environmental sensitivity of the fluorophore as the acceptor to regulate the emission intensity of the donor (Fig. 9c).

Furthermore, considering the local pH changes caused by the self-assembly process, the combination of pH probes and other techniques for the dynamic tracking of the assembly process has also attracted researchers' attention. For instance, Liu *et al.* designed a red fluorescent protein probe (pHmScarlet) with high brightness, good stability and strong pH sensitivity and used total internal reflection fluorescence microscopy (TIRFM) and FP to detect the vesicle exocytosis.[131] By combining pHmScarlet and TIRFM, they found that the mature vesicle cavity is acidic (pH is about 5.6). Also, during the process of vesicle exocytosis, the vesicle membrane and plasma membrane fuse, and the pH in the cavity instantly switches to a slightly alkaline extracellular environment (pH is about 7.4). Moreover, pHmScarlet can also detect the fluorescence intensity of intact vesicles in acidic environment, and, as a result, track and record the anchoring steps of vesicles. On further combining with the pH-sensitive fluorescent protein (pHluorin), the probe can perform two-color imaging of multiple vesicular proteins (Fig. 9d).

4.3 Light

Photosensitive probes are powerful tools for self-assembly research, which utilize optical methods to highlight the

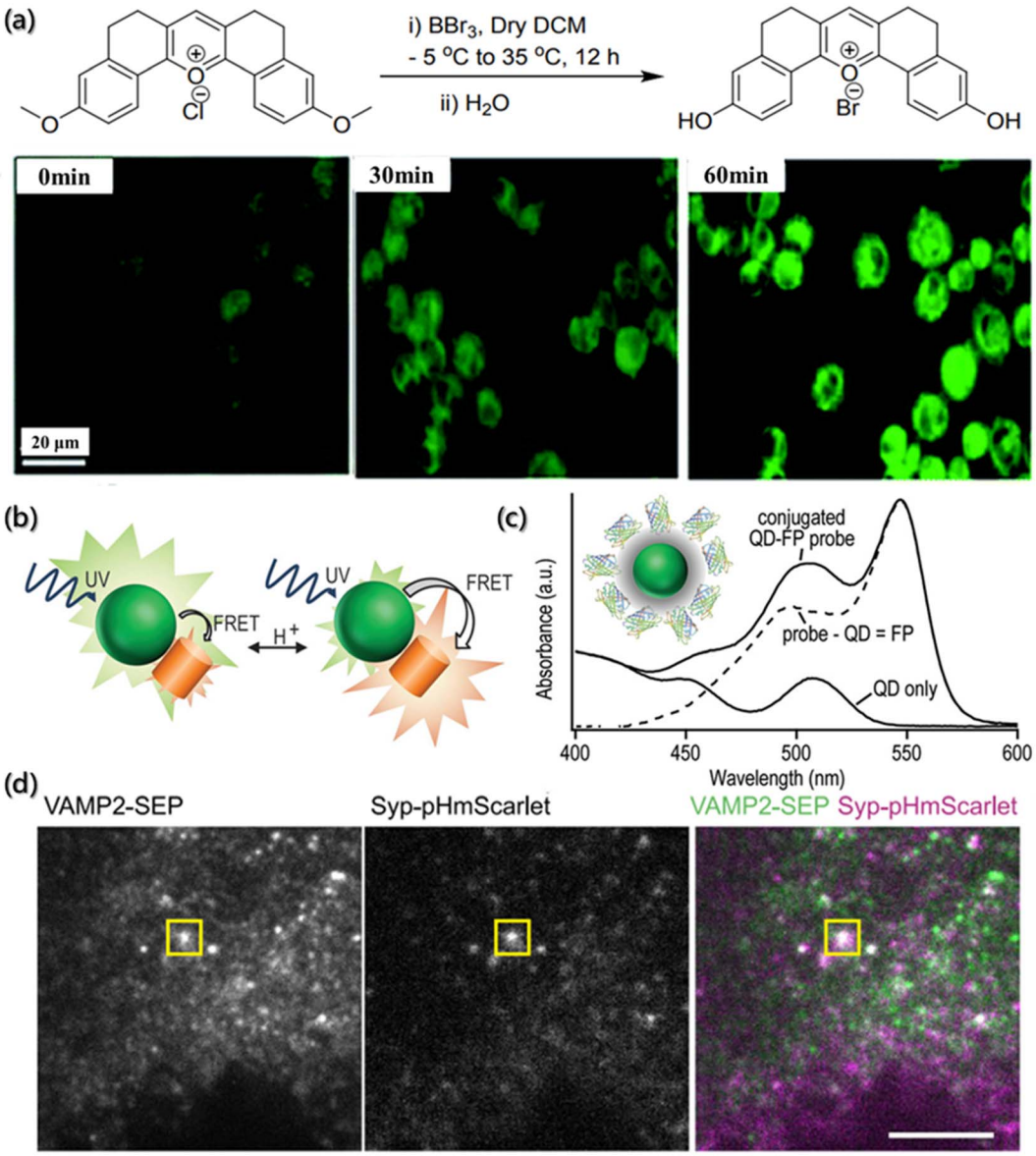

Fig. 9 pH determination of the micro-environment by a fluorescence probe. (a) Synthesis of PS-OH and fluorescence imaging of A549 cells.[129] Reproduced with permission from ref. 129. Copyright 2020, the Royal Society of Chemistry. (b) Schematic illustration of the pH-dependent energy transfer between fluorescent protein (FP) and quantum dot (QD). (c) Absorbance spectroscopy of multiple proteins bound to each QD.[130] Reproduced with permission from ref. 130. Copyright 2012, American Chemical Society. (d) TIRF of INS-1 cells expressing VAMP2-SEP (vesicle-associated membrane protein 2-superecliptic pHluorin) and Syp-pHmScarlet (synaptophysin-pHmScarlet). The vesicle fusion is indicated, scale bar is 5 μm.[131] Reproduced with permission from ref. 131. Copyright 2021, Nature Publishing Group.

changes of dynamic structure. Photosensitive probes can be divided into photoactivatable probe, photoconvertible probe and photoswitchable probe. Under light stimulation, the photoactivatable probes transfer the target from a dark state to a bright state, the photoconvertible probes change the emission wavelength, and the photoswitchable probes can be turned on and off reversibly.[133,134]

The photoactivation probes realize the function through recognizing targets, controlling the enzyme activity and activating the fluorophore by light. Generally, the "initial" probes are activated at the desired time and area, improving the contrast signal and the sensor specificity through precise space-time control.[135] For example, Zhao *et al.* designed a UV-responsive DNA probe (PBc) by installing the light cut key in MB (Fig. 10a),[136] and both ends of the PBc were labeled with quenchant (BHQ2) and fluorescent group (Cy5), respectively. When there is no light, a weak fluorescent background is generated by FRET. However, once given UV irradiation, the end of the chain modified with a quenchant would undergo a dose-dependent shift towards the target of miRNA, further leading to enhanced fluorescence signals. In addition, PBc can be used for the functionalized surface modification of nanoparticles

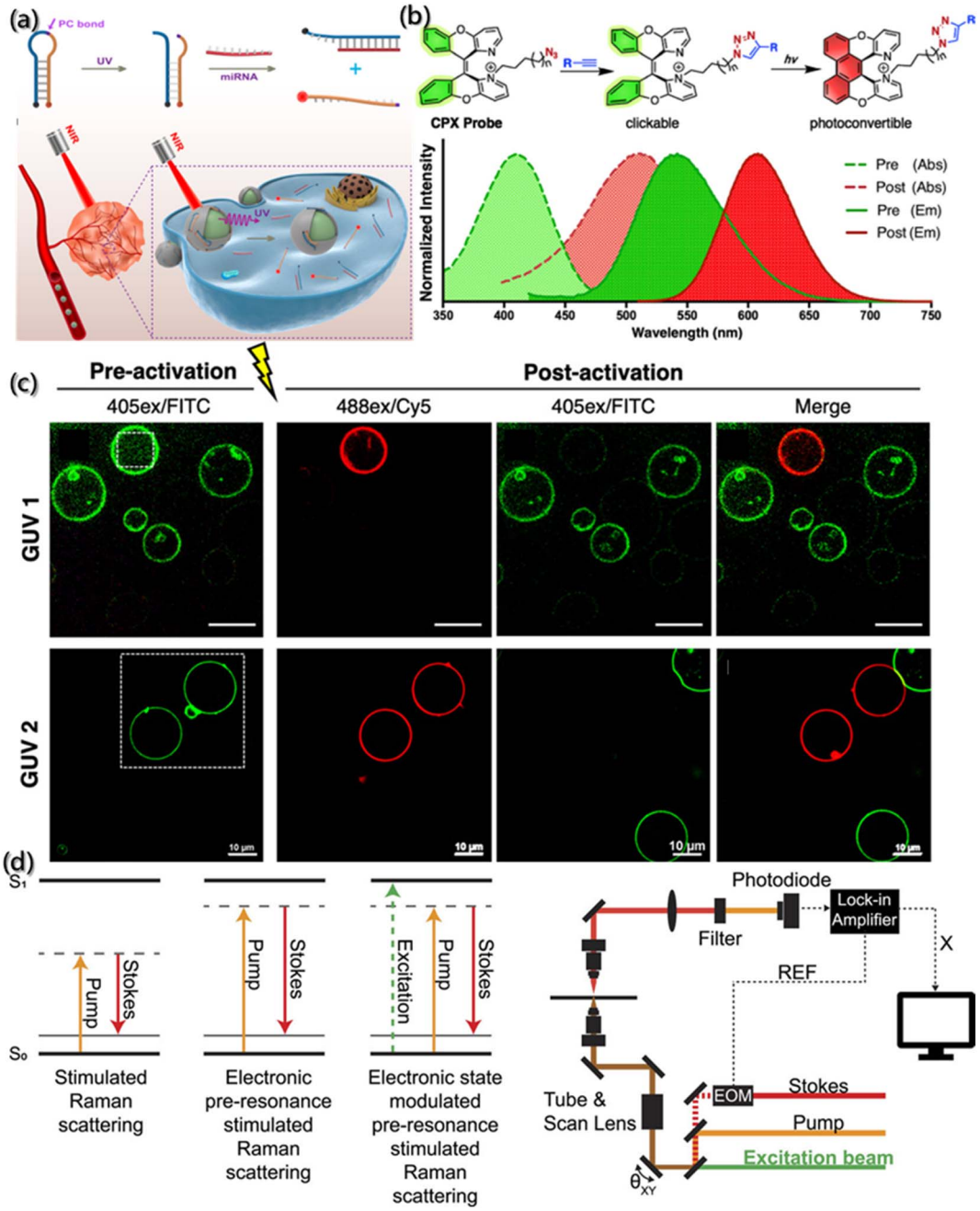

Fig. 10 Tracking of the assembly by photosensitive probes. (a) Schematic description of MB and miRNA sensing *in vivo* under NIR light.[136] Reproduced with permission from ref. 136. Copyright 2019, American Chemical Society. (b) Structure of CPX with absorption spectra (dashed line) and emission spectra (solid line) of pre-activated (green) and post-activated (red) forms. (c) Fluorescence images of vesicles with pre-activated and post-activated GUVs.[137] Reproduced with permission from ref. 137. Copyright 2019, American Chemical Society. (d) Principle and schematic description of photoswitchable electronic epr-SRS by electronic state transition (REF: reference; X: in-phase X-output of the lock-in amplifier; EOM: electro-optic modulator).[138] Reproduced with permission from ref. 138. Copyright 2021, AIP Publishing.

(UCNP), which can be used to convert low-energy near-infrared ray into high-energy ultraviolet light to conversely control the activity of PBc.

Although significant progress has been made in the gene-encoded photoactivatable fluorescent proteins, these fluorescent proteins are usually larger than targets, which may lead to adverse aggregation or functional changes of the target proteins. To overcome this challenge, Jun *et al.*[137] designed a kind of photoconvertible fluorescent small molecule (clickable and photoconvertible diazaXanthilidene (CPX)) that can transition from one fluorescence state (like green) to another state (like red) based on the photochemically permissible activation mechanism of electrocyclization or oxidation (Fig. 10b). Further application of CPX for detecting the transport of biologically related synthetic

vesicles (Fig. 10c) revealed that the selective photoconversion of giant unilamellar vesicles (GUV) labeled by CPX occurred after 440 nm laser irradiation, and the new non-photoconvert vesicles proved the transport of GUV.

With the precise regulation of fluorescence excitation and inactivation in space and time, photoswitchable molecules have greatly promoted the development of super-resolution microscopes, and the spatial resolution of optical imaging was improved to tens of nanometers. Moreover, due to the huge lifetime difference between the excited state and the non-fluorescent state, the light damage with high-power of microscope was solved. Lee *et al.* designed a photoswitchable probe for electron pre-resonance stimulated Raman scattering (epr-SRS).[138] As shown in Fig. 10d, the coupling of electrons and vibrations switches the electronic states of molecules into four different states, thereby turning on or off the ground state signals of epr-SRS. Also, the HeLa cells marked by ATTO680 azide confirmed the photoswitchable effect during epr-SRS imaging.

4.4 Polarity

As a complicated factor, polarity represents a series of non-covalent effects, such as polarizability and dipolarity, hydrogen bonding and hydration, which play pivotal roles in the assembly process.[36,139] Thus, to uncover the mysterious veil of polarity in assembly processes, the precise determination of polarity changes has been investigated. Although several analytical methods, such as spectral, electrochemical, and chromatography analysis have been developed, ideal tools for polarity detection are scarce.[140] Compared with the traditional tools, fluorescent probes are emerging as an important polarity detection tool due to their high sensitivity and selectivity, operational simplicity, real-time monitoring, high temporal–spatial resolution and non-invasiveness.

The classical strategy for designing polarity-sensitive probes is to construct a structural framework with donor and acceptor groups, thereby achieving a large dipole moment. After light absorption, this framework can ensure the transfer of charge from the donor to the acceptor, and then a highly dipolar excited state is formed. The dipolar excited state will be relaxed by the interaction with the dipoles of solvent, and thus the emission will shift to longer wavelengths in a more polar environment.[141] Yuan *et al.*[142] introduced a series of near-infrared polarity-sensitive probes with ON–OFF fluorescence switch into pluronic nanoparticles (Fig. 11a). These probes were encapsulated into the thermosensitive pluronic nanoparticles. Due to a significant variation in the emission intensity over a slight change in temperature, these probes can serve as ON–OFF fluorescence switches, and the switching ratio was proved to increase with the reduction of hydrophobic chains.

Other mechanisms can also serve as regulation mechanisms for polarity-sensitive fluorescent probes, such as twisted intramolecular charge transfer (TICT) and excited state intramolecular proton transfer (ESIPT).[144,145] Typical examples are 3-hydroxyflavone derivatives. After the ESIPT reaction, these derivatives exhibit intense solvatochromism with double emission peaks. Ryder *et al.* used a variety of fluorescent probes (4′-diethylamino-3-hydroxyflavone (FE), 5,6-benzo-4′-diethylamino-3-hydroxyflavone (BFE), and 4′-diethylamino-3-hydroxy-7-methoxyflavone (MFE)) to evaluate the polarity of thermosensitive copolymer films (Fig. 11b).[143] It was found that the increase in the hydrophobicity would result in a decrease in the ratio of the two emission intensities (I_{N*}/I_{T*}). Therefore, the composition of copolymer is closely related to the probe-doped copolymer films.

4.5 Local viscosity fluctuations

During the self-assembly process, viscosity is also an important micro-environment parameter, which can reflect the flow state of building blocks and aggregates in the system, play a significant role in the mass and energy transfer, as well as the molecular interactions.[146–148] The traditional viscosity measurement tools based on the hysteresis principle are difficult to realize dynamic detection, which poses a great challenge to viscosity measurement in the self-assembly process. Researchers have found that the orientation of the absorption transition moment (M_A) and emission transition moment (M_B) of fluorescent molecules depend on their structure. Although the ground states of all fluorescent molecules in homogeneous solution are randomly oriented, once excited by the polarized light with the incident photoelectron parallel to M_A, the orientation of excited fluorescent molecules is no longer random, and the emitted light is also polarized. The degree of polarization depends on the diffusion of molecules, which is related to the viscosity of environment and the size and shape of fluorescent molecules.[149,150] Therefore, fluorescence probes can be used for determining the local viscosity of assembly systems.

Zheng *et al.* synthesized a near infrared fluorescence probe (Mito-NV) (Fig. 12a) based on the twisted intramolecular charge transfer theory using 4-pyridine acetonitrile as the electron acceptor and dimethylaniline as the electron donor, respectively.[151] The Mito-NV probe is sensitive to viscosity, and its fluorescence intensity exhibits good linear correlation with viscosity. The maximum absorption peak of Mito-NV in water is located at 520 nm, while the maximum peak in glycerol is located at 685 nm. The large Stokes shift (155 nm) effectively avoids interference form background fluorescence. The probe rotor rotates with high speed at low viscosity and generates very weak fluorescence. On the contrary, the rotation of the rotor is suppressed at high viscosity, resulting in strong fluorescence signal from Mito-NV.

In addition, the diversity and complexity of the system during assembly have put forward higher and extensive requirements on the fluorescent probes so that more researchers are paying attention to multi-functional probes with multiple environmental parameters detection capabilities.[153,154] Song *et al.* designed a dual-response fluorescent probe for cancer imaging, which can simultaneously monitor the pH and viscosity,[152] based on the acid-activated transformation of iminopyrrol and aminopyrrol, and twisted intramolecular charge shuttle (TICS) fluorescence sensing mechanism (Fig. 12b). Moreover, the aniline group of the probe is not only a pH-responsive site but also viscosity-responsive. Commonly, in an alkaline environment with any viscosity gradient, the probe molecules are in the form of iminopyrrosine without obvious absorption in the visible

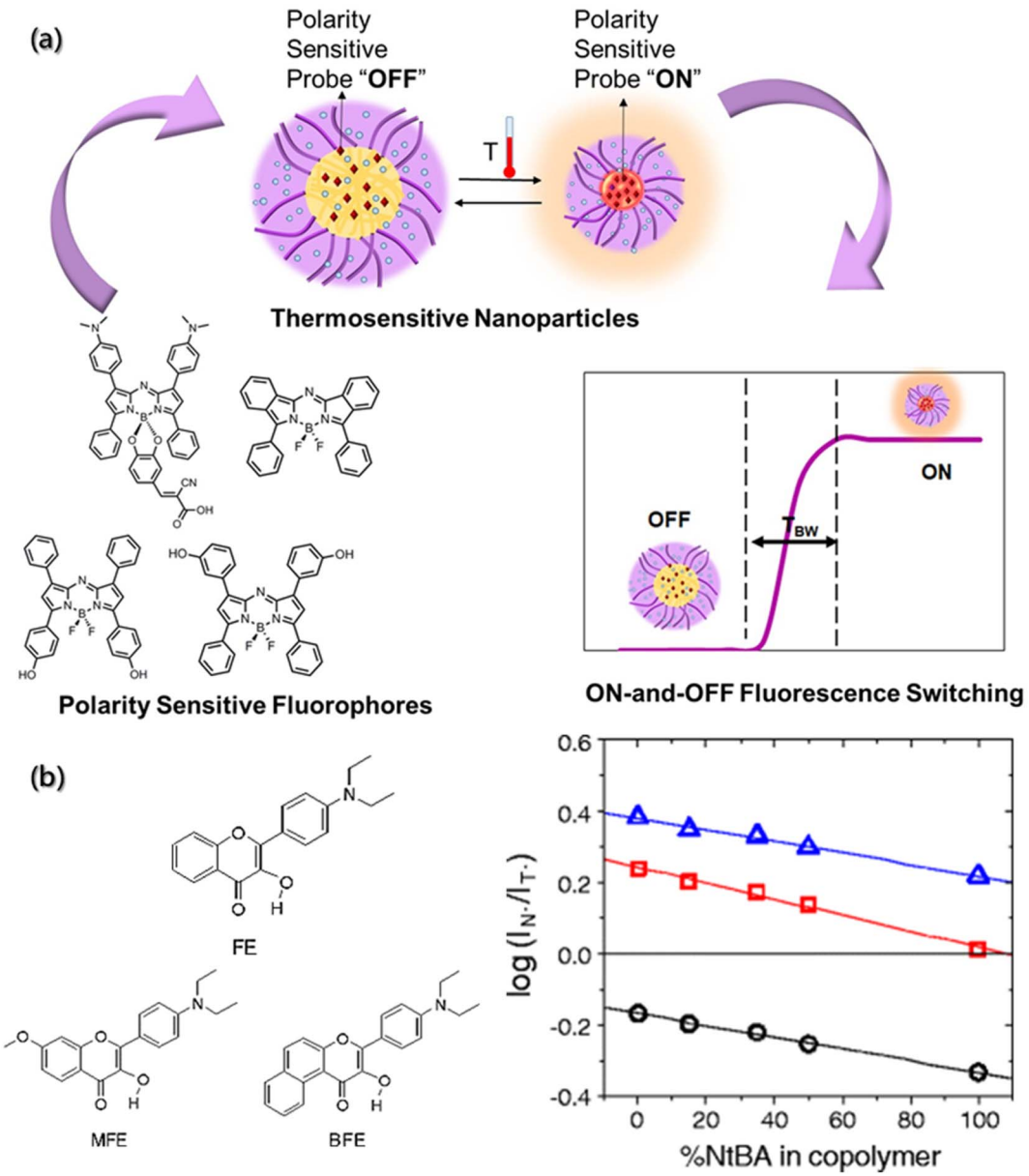

Fig. 11 Polarity determination of micro-environment by a fluorescence probe. (a) Near-infrared polarity sensitive probes with ON-and-OFF fluorescence switching in pluronic nanoparticles.[142] Reproduced with permission from ref. 142. Copyright 2020, Multidisciplinary Digital Publishing Institute. (b) Chemical structures of hydroxyflavone derivatives for polarity sensitive probes, and the plot of log(I_{N*}/I_{T*}) *versus* % of hydrophilic component for the MFE, FE, BFE-doped films.[143] Reproduced with permission from ref. 143. Copyright 2010, Nature Publishing Group.

region. However, in acidic and low viscosity environments, the probe molecules take the form of aminopyrrole and have strong absorption in the visible region. Meanwhile, the rotation of aniline groups at the excited state would cause TICS, making it unable to generate fluorescence. However, in acidic and high viscosity environment, the probe molecules are in the aminopyrrole form, which can inhibit the rotation of the aniline group and limit TICS, resulting in strong fluorescence.

4.6 Field-stimulation response

Although response probes based on temperature, pH and light have shown excellent intensity and resolution, the image resolution sharply declines under extreme conditions, such as the deep tracking of non-invasive living animals. Some compound probes, like field-stimulation response, may provide stronger fluorescence signal.

Photoacoustic (PA) probes, produced by coupling NIR and ultrasonic readout, benefiting from rich contrast, high resolution, and deep tissue penetration, have shown good prospects in biomedical imaging.[155] The PA probe design should consider the following principles: (1) the excited light generated by the probe after absorbing NIR must have considerable penetration ability. (2) The PA signal produced by the probe for detection should be strong. And (3) The absorbance overlaps between the

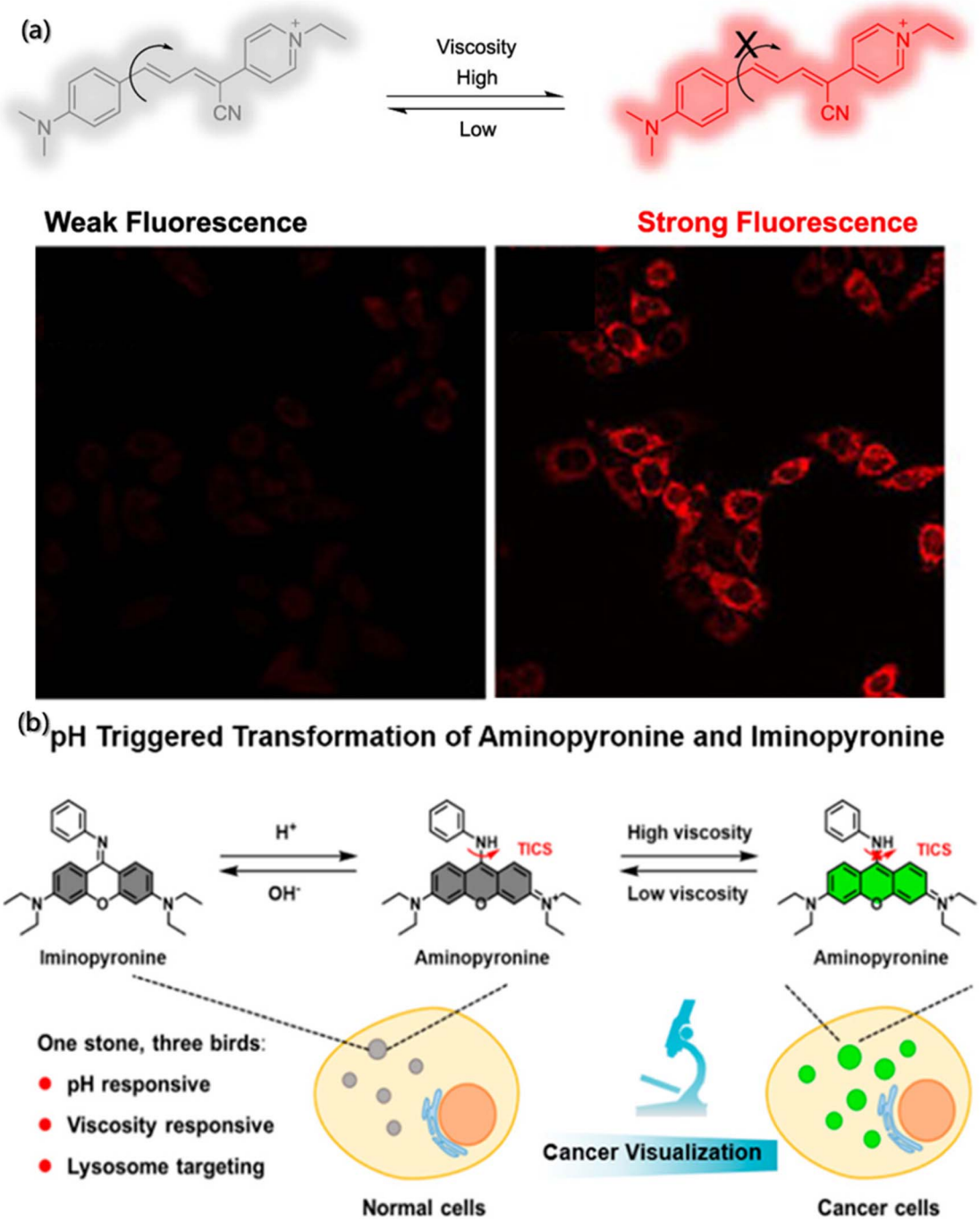

Fig. 12 Determination of local viscosity by fluorescence probes. (a) Structure and action mechanism of Mito-NV.[151] Reproduced with permission from ref. 151. Copyright 2021, American Chemical Society. (b) Structure and action mechanism of the probe under pH and viscosity change.[152] Reproduced with permission from ref. 152. Copyright 2021, American Chemical Society.

probe and the substrate should be less. Zhou *et al.* synthesized conformationally-restricted analogues of hypoxia-responsive probe/product pair (HyP-1/red-HyP-1) and constructed the conformationally-restricted aza-BODIPY (CRaB) platform (Fig. 13a).[156] As shown in Fig. 13b, the theoretical ratiometric response of the three probes was improved by 2–8 times *in vitro*, showing great potential for PA response. Besides, the detection of the hypoxic tumor model demonstrated the potential of the CRaB scaffold *in vivo*.

In order to improve the detection sensitivity of ochratoxin A (OTA), Yao *et al.* enhanced the signal and reduced the noise based on rolling circular amplification (RCA) and magnetic purification.[157] As shown in Fig. 13c and d, the aptamer of OTA was designed as the fragment of RCA primers and fixed on

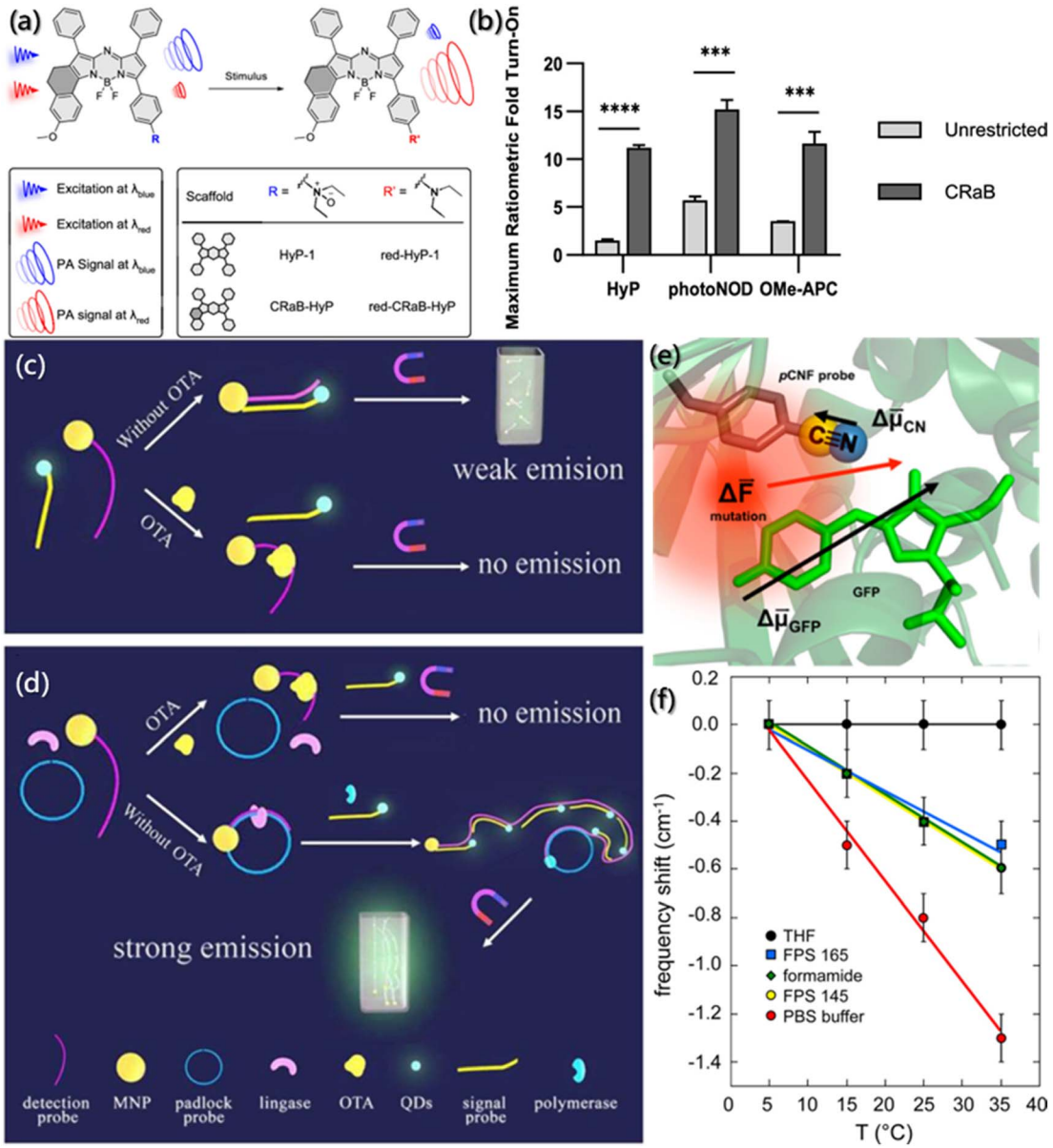

Fig. 13 Tracking of assembly by field effect fluorescent probes. (a) Schematic description and structure of stimulus-responsive PA probes. (b) Theoretical ratiometric fold turn-on of CRaB probes and corresponding unrestricted counterparts.[156] Reproduced with permission from ref. 156. Copyright 2019, American Chemical Society. (c and d) The integrated platform for the detection of OTA.[157] Reproduced with permission from ref. 157. Copyright 2015, Elsevier. (e) Close-up view of green fluorescent protein. Arrows represent the approximate magnitudes and directions of difference dipole moments. (f) Changes in the nitrile stretching frequency in different solutions and pCNF position as a function of temperature.[158] Reproduced with permission from ref. 158. Copyright 2016, American Chemical Society.

magnetic nanoparticles (MNP). An external magnetic field was applied to purify the mixture in the sensor system to remove the residual quantum dots (QDs)-labeled probe and reduce the interference of the background fluorescent noise. Also, the RCA could tremendously increase the hybridization sequence of QDs-labeled probes, thereby further increasing the sensing response signal. For the probes with the best sensing performance after systematic optimization, the response sensing range for OTA detection was improved by 3 orders of magnitude, and the detection limit was as low as 0.13 ppt, which is 10 000 times higher than those of traditional methods.

Furthermore, based on the specificity of vibrational oscillation to the micro-environment, nitrile functionality probes were generally used as the reporter of electric field caused by vibrational Stark effect (VSE) spectroscopy. VSE spectroscopy has been usually used to investigate the assembly kinetics, conformational folding and local static electricity.[159,160] However, due to the large dipole moment of the ground state and the strong hydrogen bonding ability of nitrile groups, the detection of the electric field is usually very complex. Slocum *et al.* incorporated *p*-cyanophenylalanine (*p*CNF) residues into green fluorescent protein (GFP),[158] and it perfectly solved the external disturbance

effect generated when nitrile acted as the Stark effect probe, exploiting the inherent linear sensitivity of GFP to the electric field (Fig. 13e). As shown in Fig. 13f, even if the hydrogen bonding was formed between the probes and the solvent, the change in the electric field monitored by the vibrating probe and the natural fluorophore was monotonous and linear.

5. Tracking of self-assembly kinetics

The self-assembly process is driven by both thermodynamics and kinetics, and understanding the kinetics of self-assembly is beneficial for predicting the assembly behavior and designing hierarchical structures.[161,162] However, due to a lack of effective approaches for morphological evolution tracking during the assembly process, few researchers have systematically considered the kinetic process since existing research was mostly focused on the structural changes between aggregates.[7] The proposal of a fluorescent probe provides a new idea for kinetic characterization.

Generally, building blocks with fluorescent groups are usually designed to track the self-assembled process and to further obtain kinetics data as the emission and absorption spectra of fluorescent groups are simple to determine and environmentally sensitive. Aratsu *et al.* designed a series of barbituric acid molecules to explore the self-assembly mechanism.[27] They found that barbituric acid can be assembled into six-membered complexes similar to rosettes by complementary hydrogen bonding, which are further assembled into a helicoid through the π–π interaction between the naphthalene rings (Fig. 14a). The increase in UV absorption was considered to be the result of self-assembly due to the electron complementarity between naphthalene chromophores, which was confirmed by the change in the fluorescence spectrum with the aggregation of the naphthalene ring (Fig. 14b and c). Moreover, the absorption peak at 470 nm was described as the function of kinetics, and the kinetic mechanisms of self-assembly, spiralization and dissociation were obtained (Fig. 14d). In addition, the kinetic results of fluorophore characterization were also confirmed by time-dependent dynamic light scattering (DLS) and atomic force microscopy (AFM) (Fig. 14e and f).

However, for several building blocks without fluorescent groups, it is also necessary and crucial to find convenient and reliable methods for process detection during self-assembly. Fortunately, 8-anilinonaphthalene-1-sulfonic acid (ANS), as a fluorescent probe, exhibits high affinity for hydrophobic surfaces. In the low polarity region, when ANS binds to the

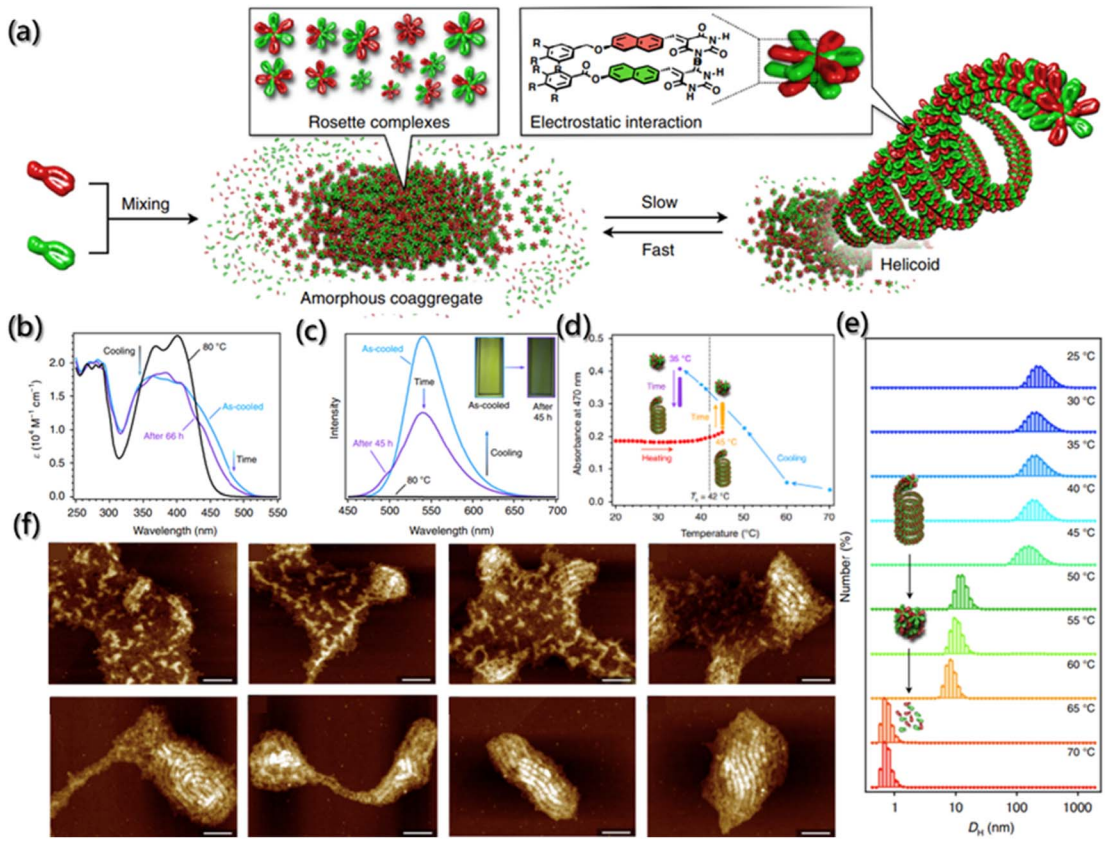

Fig. 14 Co-assembly kinetics of barbituric acid. (a) Schematic illustration of the supramolecular copolymerization of barbituric acid into a helicoid. (b and c) The absorption and fluorescence emission spectra of the 1 : 1 mixture of barbituric acid upon cooling, and the subsequent time-dependent change. (d) Absorbance at 470 nm as a function of temperature during cooling and subsequent aging process. (e) DLS of the helicoids from 25 to 70 °C. (f) AFM images during the transition of the 1 : 1 mixture of barbituric acid into helicoids. Scale bars are 100 nm.[27] Reproduced with permission from ref. 27. Copyright 2020, Nature Publishing Group.

surfaces of the aggregate, its spectrum undergoes blue shifts and fluorescence intensity enhancement. Therefore, ANS has received extensive attention in the field of assembly process detection.[163] Laishram *et al.* incorporated ANS as the polarity sensitive fluorescent probe into the mixed gel (CaCh2) of calcium salt (Ca^{2+}) and sodium cholate (NaCh) to monitor the self-assembly process of the gel (Fig. 15a).[28] They found that the bound ANS was released from the hydrophobic pocket of NaCh into the bulk medium of water, causing some characteristic changes in emission during the assembly of gels. The spectral emission changes of ANS at 500 nm was carried out for the kinetic detection of CaCh2, and the Watzky–Finke model of autocatalytic nucleation–elongation was used to fit the nonlinear kinetic curves with good fitting results (Fig. 15b and c). In addition, with the addition of gel seeds, the secondary nucleation rate constant increased with the increase in the seed proportion. Moreover, the surface-catalyzed secondary nucleation triggered the transverse growth and winding of the fiber by the hydrogen bonding or hydrophobic interaction between the fiber surface and free monomers, forming the bundle fibers (Fig. 15d).

In addition, the existence of multiple intermediates and many possible processes certainly challenge the dynamic detection of self-assembly. The high sensitivity of FRET technology promotes the detection of interacting substances at nanomolar concentrations, and it is simple and easy to detect samples in the solution. Hence, the change in the individual components and the assemblies can be observed directly by FRET. FRET is an ideal technique for the real-time monitoring of self-assembly processes and dynamics, with high sensitivity and efficiency. Huang designed and synthesized dipyridyl ligand and diplatinum(II) units labeled with 7-(diethylamino)-coumarin and rhodamine as the donor and the acceptor fluorophore (Fig. 16a), which formed the metallacycles through coordination-driven self-assembly (Fig. 16b).[164] FRET was used to monitor the process of metallacycles self-assembly driven by coordination interactions in real time. Over time, an apparent increase in the acceptor (rhodamine) emissions was observed to be accompanied by a decrease in the donor (coumarin) emissions until equilibrium was reached. The ratio of the fluorescence intensity of rhodamine at 602 nm to the fluorescence intensity of coumarin at 467 nm increased until equilibrium (Fig. 16c and d). Besides, the enhancement of fluorescence intensity ratios was almost linear with the self-assembly time, and the self-assembly of metallacycles could be monitored in real time.

Compared with one-step FRET, multistep FRET systems, incorporating two or more fluorophores, have received

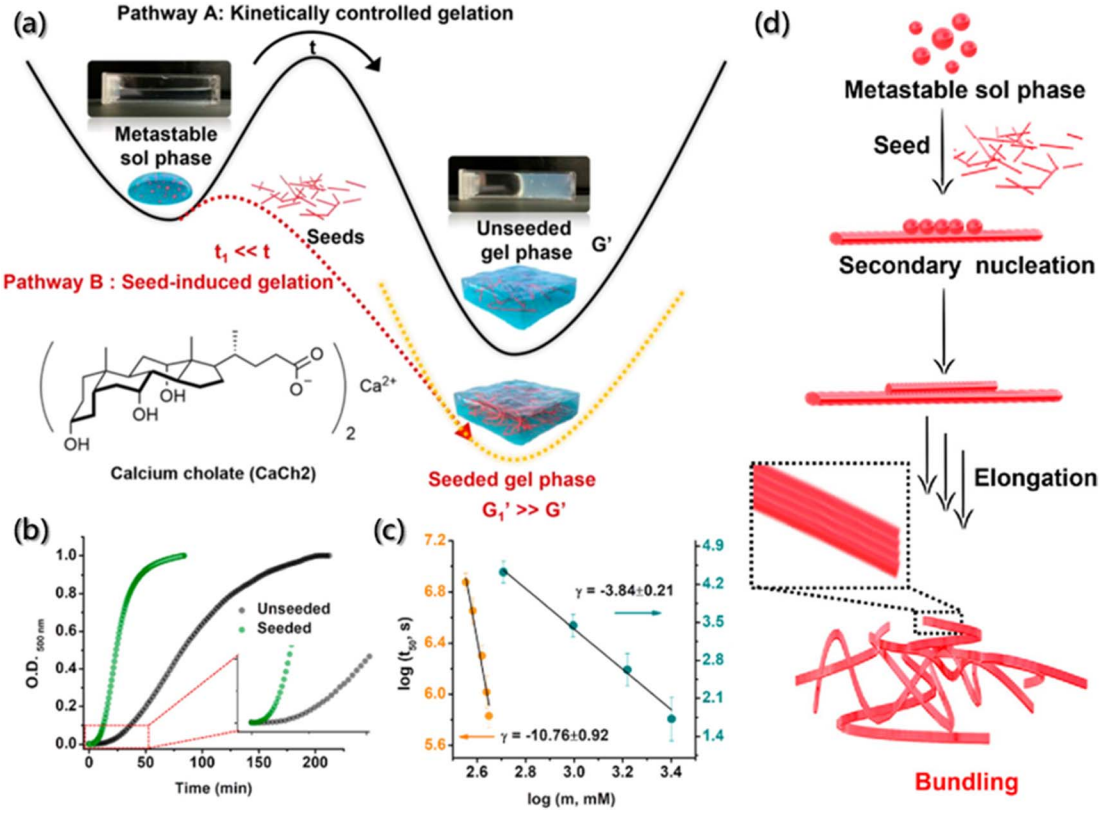

Fig. 15 Secondary nucleation-triggered assembly kinetics of CaCh2. (a) Schematic illustration of the kinetically-controlled supramolecular assembly of CaCh2. (b) Assembly kinetic profiles with and without the seed of CaCh2 by probing the optical density at 500 nm. (c) Double logarithm plots of half-time (t_{50}) (the time of 50% completion of the assembly process) with the CaCh2 concentration for unseeded and seeded assembly. (d) Schematic illustration of the secondary nucleation process during the seed-induced assembly.[28] Reproduced with permission from ref. 28. Copyright 2022, American Chemical Society.

increasing attention for monitoring assemblies.[166,167] Multistep FRET systems, especially the two-step FRET, offer several advantages over one-step FRET, such as higher efficiency of long-range energy transfer, larger Stokes shift even in the absence of spectral overlap, and better detection sensitivity for acceptor fluorescence. Therefore, multistep FRET systems

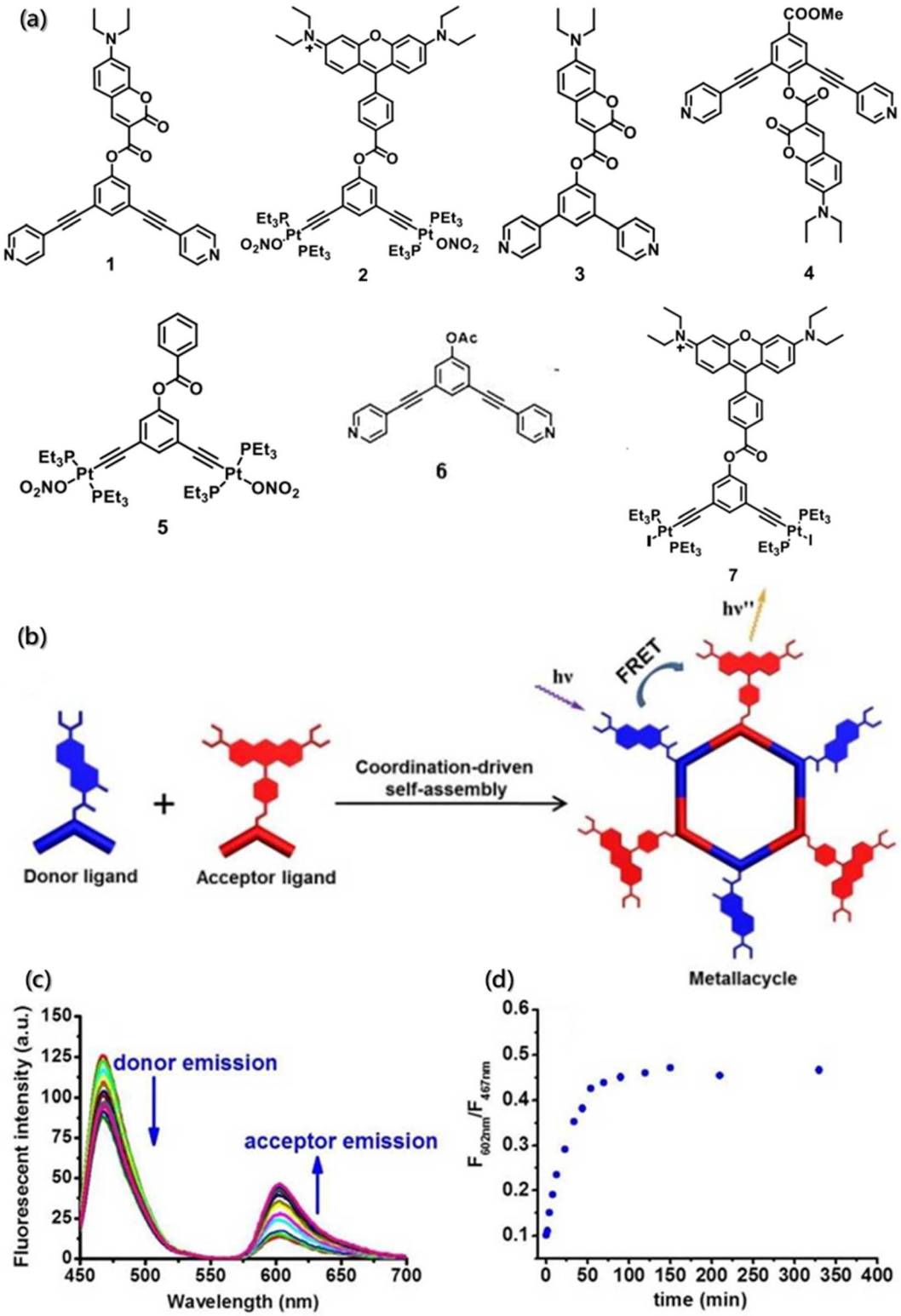

Fig. 16 (a) Structure of building blocks 1–7. (b) Coordination-driven self-assembly of the donor ligand and the acceptor ligand. (c) Time-dependent emission spectra of the self-assembly system. (d) Change in the ratio of the fluorescence intensity with time.[164] Reproduced with permission from ref. 164. Copyright 2017, American Chemical Society.

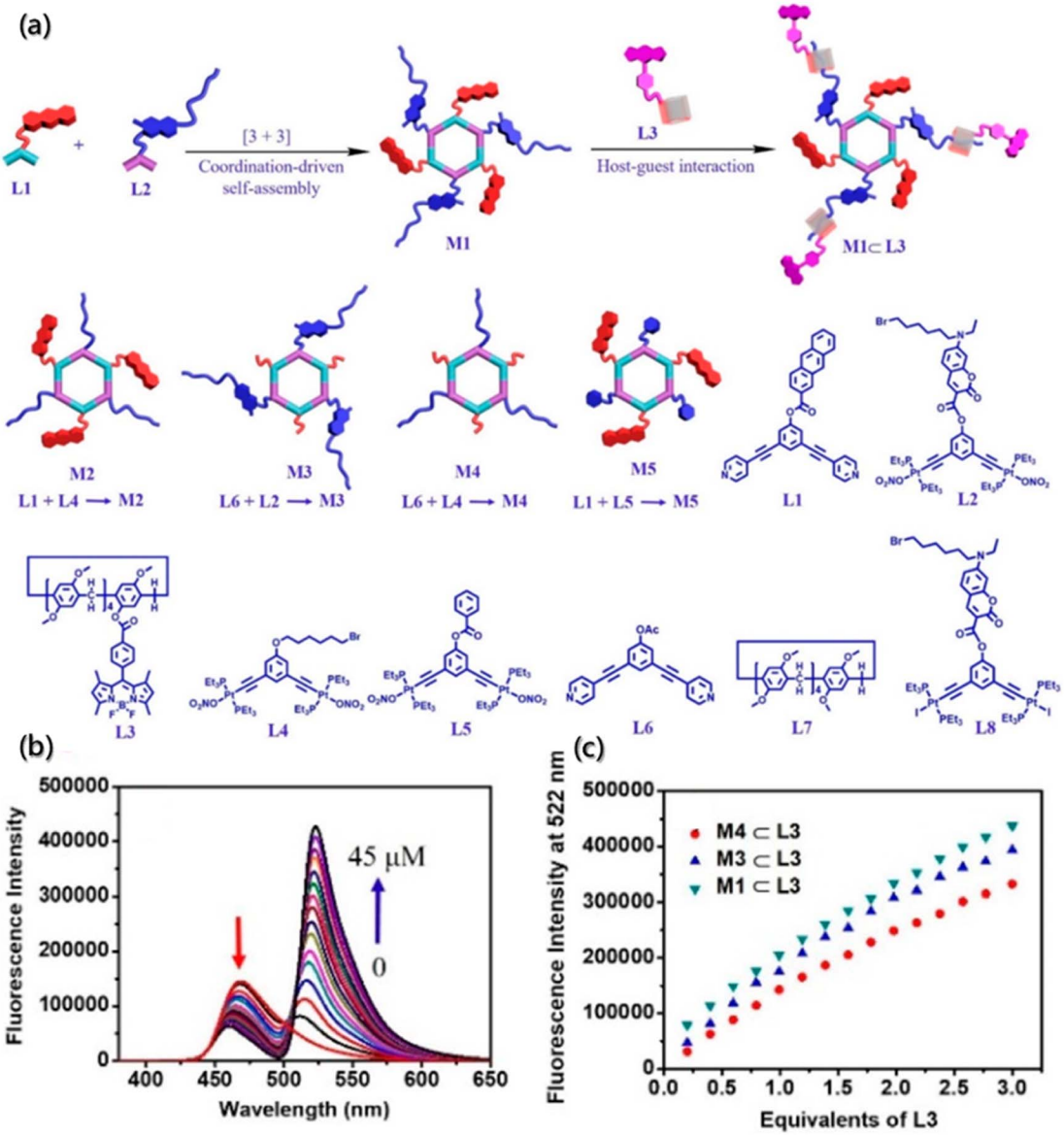

Fig. 17 Orthogonal self-assembly of a two-step fluorescence-resonance energy transfer system. (a) Self-assembly of M1–M5 metallacycles, M1 ⊂ L3 supramolecular system, and chemical structures of L1–L8 building blocks. (b) Emission spectra of metallacycle upon titration of the building block. (c) Fluorescence intensity changes of metallacycles upon titration of the building block.[165] Reproduced with permission from ref. 165. Copyright 2021, American Chemical Society.

significantly improve the possibility of realizing energy transfer or monitoring inter- and intramolecular interactions generated exceeding 10 nm and extend the excitation wavelength range for fluorescence lifetime measurements.[168] Through orthogonal self-assembly based on macrocycle host–guest and metal–ligand coordination interactions, Yang constructed a supramolecular system containing coumarin, anthracene, and BODIPY moieties (Fig. 17a) and achieved the two-step energy transfer from anthracene to coumarin and then to BODIPY moieties.[165] Further investigations according to the two-step FRET processes of the orthogonal self-assembly indicated that the gradual addition of L3 to a solution of hexagonal metallacycles could reduce the fluorescence emission at 465 nm and increase the intensity of fluorescence emission at 522 nm simultaneously (Fig. 17b and c) under the excitation of anthracene.

6. Conclusions and outlook

Self-assembly, as well as disassembly, is a ubiquitous process in nature, and it is essential for controlling and regulating the transformation of substances from simple to complex and between disorder and order. Although multiple methods have been applied to study self-assembly processes, the vast majority of methods can only indirectly obtain self-assembly information. Considering the unique ability and exceptional properties of fluorescence probes for *in situ* obtaining real-time, non-destructive, sensitive, and efficient data and information, the

important tracking role and potential applications of fluorescent probes during self-assembly process was reviewed in this work. Some novel and/or traditional fluorescent probe regulating modes were introduced to help understand the working mechanisms of probes. Also, the fluorescent molecules as tracer probes to track the self-assembly process of chemical entities, including direct imaging, description of aggregate properties, and kinetic characterization or dynamic monitoring, were systematically and comprehensively summarized. It is well known that tracking is the key to understanding the mechanisms of self-assembly, and a full understanding of self-assembly mechanisms can help to accurately control the self-assembly process. Besides some stimulus-responsive fluorescent probes, the useful tools for understanding the micro-environment during the self-assembly process were also introduced.

Nevertheless, there are still some bottlenecks and challenges that need to be overcome to make better use of these fluorescent probes in self-assembly. First of all, although fluorescent probes have been widely used for the self-assembly analysis of macromolecules *in vivo*, more probes suitable for small molecular systems are expected to be proposed. The key to this issue is to design recognition groups so that probes can act on supramolecular aggregates with a small amount of specificity. For instance, the double-locked probe, covering two or multiple sequential triggers in a single system, could be sequentially activated by two or more analytes by cascading.[169,170] With the help of these double-locked probes, measurement uncertainties (like reactivity discrepancies and spectral crosstalk) caused by several identification groups can be avoided. Secondly, the current fluorescent probes may not exhibit desired selectivity and sensitivity for some new systems that are constantly discovered, and parameters in self-assembly need to be accurately measured so that researchers need to develop more fluorescent probes to better monitor the properties of the aggregates and control the assembly direction of new systems. Finally, although fluorescent probes are widely used owing to low dosage and non-destructive testing, the fluorescent groups and recognition groups inevitably affect the assembly of aggregates. Currently, some physical and chemical methods are used to remove the fluorescent probes, such as adsorption, coagulation–flocculation, electrochemical methods, oxidation, and biological reduction.[171–173] However, the limitations of these methods and possible by-product formation need to be recognized. Therefore, avoiding the influence of probe molecules on the assembly or developing a real non-invasive method for probe removal is also a future research direction. Overall, fluorescent probes provide a powerful tool for self-assembly process analysis and monitoring, although there is still more work to be done. We believe that fluorescent probes can significantly promote our understanding of self-assembly.

Author contributions

Xiongtao Ji: conceptualization, methodology, visualization, writing – original draft. Na Wang: funding acquisition, supervision, writing – review & editing. Jingkang Wang: funding acquisition. Ting Wang: supervision. Xin Huang: supervision. Hongxun Hao: funding acquisition, supervision, writing – review & editing.

Conflicts of interest

There are no conflicts to declare.

Acknowledgements

The authors are very grateful to the financial supported from the National Natural Science Foundation of China [No. 21978201 and 22108196].

References

1 J. V. I. Timonen, M. Latikka, L. Leibler, R. H. A. Ras and O. Ikkala, Switchable Static and Dynamic Self-Assembly of Magnetic Droplets on Superhydrophobic Surfaces, *Science*, 2013, **341**, 253–257.
2 J. Liu, J. Tang, Z. Tong, G. Teng and D. Yang, DNA-guided self-assembly in living cells, *Iscience*, 2023, **26**, 106620.
3 J. Gao, J. Zhan and Z. Yang, Enzyme-Instructed Self-Assembly (EISA) and Hydrogelation of Peptides, *Adv. Mater.*, 2020, **32**, 1805798.
4 S. Cao, J. Shao, L. K. E. A. Abdelmohsen and J. C. M. van Hest, Amphiphilic AIEgen-polymer aggregates: Design, self-assembly and biomedical applications, *Aggregate*, 2022, **3**, e128.
5 A. C. Mendes, E. T. Baran, R. L. Reis and H. S. Azevedo, Self-assembly in nature: using the principles of nature to create complex nanobiomaterials, *Wiley Interdiscip. Rev.: Nanomed. Nanobiotechnology.*, 2013, **5**, 582–612.
6 W. Jiang, Y. Zhou and D. Yan, Hyperbranched polymer vesicles: from self-assembly, characterization, mechanisms, and properties to applications, *Chem. Soc. Rev.*, 2015, **44**, 3874–3889.
7 Y. Lu, J. Lin, L. Wang, L. Zhang and C. Cai, Self-Assembly of Copolymer Micelles: Higher-Level Assembly for Constructing Hierarchical Structure, *Chem. Rev.*, 2020, **120**, 4111–4140.
8 Z. Wang, Y. Guo and Y. Xianyu, Applications of self-assembly strategies in immunoassays: A review, *Coord. Chem. Rev.*, 2023, **478**, 214974.
9 P. Pan, X. Chen, K. Metavarayuth, J. Su and Q. Wang, Self-assembled supramolecular systems for bone engineering applications, *Curr. Opin. Colloid Interface Sci.*, 2018, **35**, 104–111.
10 P. R. Banerjee, A. N. Milin, M. M. Moosa, P. L. Onuchic and A. A. Deniz, Reentrant Phase Transition Drives Dynamic Substructure Formation in Ribonucleoprotein Droplets, *Angew. Chem., Int. Ed.*, 2017, **56**, 11354–11359.
11 Y.-T. Kao, K. L. Gonzalez and B. Bartel, Peroxisome Function, Biogenesis, and Dynamics in Plants, *Plant Physiol.*, 2018, **176**, 162–177.
12 Y. Lin, D. S. W. Protter, M. K. Rosen and R. Parker, Formation and Maturation of Phase-Separated Liquid

Droplets by RNA-Binding Proteins, *Mol. Cell*, 2015, **60**, 208–219.

13 C. Pohl, G. Effantin, E. Kandiah, S. Meier, G. Zeng, W. Streicher, D. R. Segura, P. H. Mygind, D. Sandvang, L. A. Nielsen, G. H. J. Peters, G. Schoehn, C. Mueller-Dieckmann, A. Noergaard and P. Harris, pH- and concentration-dependent supramolecular assembly of a fungal defensin plectasin variant into helical non-amyloid fibrils, *Nat. Commun.*, 2022, **13**, 3162.

14 F. Araste, A. Aliabadi, K. Abnous, S. M. Taghdisi, M. Ramezani and M. Alibolandi, Self-assembled polymeric vesicles: Focus on polymersomes in cancer treatment, *J. Controlled Release*, 2021, **330**, 502–528.

15 M. Delfi, R. Sartorius, M. Ashrafizadeh, E. Sharifi, Y. Zhang, P. De Berardinis, A. Zarrabi, R. S. Varma, F. R. Tay, B. R. Smith and P. Makvandi, Self-assembled peptide and protein nanostructures for anti-cancer therapy: Targeted delivery, stimuli-responsive devices and immunotherapy, *Nano Today*, 2021, **38**, 101119.

16 A. Levin, T. A. Hakala, L. Schnaider, G. J. L. Bernardes, E. Gazit and T. P. J. Knowles, Biomimetic peptide self-assembly for functional materials, *Nat. Rev. Chem*, 2020, **4**, 615–634.

17 C. D. Spicer, C. Jumeaux, B. Gupta and M. M. Stevens, Peptide and protein nanoparticle conjugates: versatile platforms for biomedical applications, *Chem. Soc. Rev.*, 2018, **47**, 3574–3620.

18 T. Douglas and Y. Wang, Bioinspired Approaches to Self-Assembly of Virus-like Particles: From Molecules to Materials, *Acc. Chem. Res.*, 2022, **55**, 1349–1359.

19 Y. Gao, J. Zhao, Z. Huang, T. K. Ronson, F. Zhao, Y. Wang, B. Li, C. Feng, Y. Yu, Y. Cheng, D. Yang, X.-J. Yang and B. Wu, Hierarchical Self-Assembly of Adhesive and Conductive Gels with Anion-Coordinated Triple Helicate Junctions, *Angew. Chem., Int. Ed.*, 2022, **61**, e202201793.

20 I. Insua, J. Bergueiro, A. Mendez-Ardoy, I. Lostale-Seijo and J. Montenegro, Bottom-up supramolecular assembly in two dimensions, *Chem. Sci.*, 2022, **13**, 3057–3068.

21 A. Aliprandi, M. Mauro and L. De Cola, Controlling and imaging biomimetic self-assembly, *Nat. Chem.*, 2016, **8**, 10–15.

22 P. F. Damasceno, M. Engel and S. C. Glotzer, Predictive Self-Assembly of Polyhedra into Complex Structures, *Science*, 2012, **337**, 453–457.

23 J. Kim, Z. Ou, M. R. Jones, X. Song and Q. Chen, Imaging the polymerization of multivalent nanoparticles in solution, *Nat. Commun.*, 2017, **8**, 761.

24 W. C. Lee, B. H. Kim, S. Choi, S. Takeuchi and J. Park, Liquid Cell Electron Microscopy of Nanoparticle Self-Assembly Driven by Solvent Drying, *J. Phys. Chem. Lett.*, 2017, **8**, 647–654.

25 H.-G. Liao, L. Cui, S. Whitelam and H. Zheng, Real-Time Imaging of Pt3Fe Nanorod Growth in Solution, *Science*, 2012, **336**, 1011–1014.

26 Y. Liang, X. Zhao, T. Hu, B. Chen, Z. Yin, P. X. Ma and B. Guo, Adhesive Hemostatic Conducting Injectable Composite Hydrogels with Sustained Drug Release and Photothermal Antibacterial Activity to Promote Full-Thickness Skin Regeneration During Wound Healing, *Small*, 2019, **15**, 1900046.

27 K. Aratsu, R. Takeya, B. R. Pauw, M. J. Hollamby, Y. Kitamoto, N. Shimizu, H. Takagi, R. Haruki, S.-i. Adachi and S. Yagai, Supramolecular copolymerization driven by integrative self-sorting of hydrogen-bonded rosettes, *Nat. Commun.*, 2020, **11**, 1623.

28 R. Laishram, S. Sarkar, I. Seth, N. Khatun, V. K. Aswal, U. Maitra and S. J. George, Secondary Nucleation-Triggered Physical Cross-Links and Tunable Stiffness in Seeded Supramolecular Hydrogels, *J. Am. Chem. Soc.*, 2022, **144**, 11306–11315.

29 J. Matern, Y. Dorca, L. Sanchez and G. Fernandez, Revising Complex Supramolecular Polymerization under Kinetic and Thermodynamic Control, *Angew. Chem., Int. Ed.*, 2019, **58**, 16730–16740.

30 Y. Shao, H. Jia, T. Cao and D. Liu, Supramolecular Hydrogels Based on DNA Self-Assembly, *Acc. Chem. Res.*, 2017, **50**, 659–668.

31 L. Xu, H. Wang, Z. Chu, L. Cai, H. Shi, C. Zhu, D. Pan, J. Pan, X. Fei and Y. Lei, Temperature-Responsive Multilayer Films of Micelle-Based Composites for Controlled Release of a Third-Generation EGFR Inhibitor, *ACS Appl. Polym. Mater.*, 2020, **2**, 741–750.

32 X. Yan, D. Xu, X. Chi, J. Chen, S. Dong, X. Ding, Y. Yu and F. Huang, A Multiresponsive, Shape-Persistent, and Elastic Supramolecular Polymer Network Gel Constructed by Orthogonal Self-Assembly, *Adv. Mater.*, 2012, **24**, 362–369.

33 L. Yuan, W. Lin, K. Zheng, L. He and W. Huang, Far-red to near infrared analyte-responsive fluorescent probes based on organic fluorophore platforms for fluorescence imaging, *Chem. Soc. Rev.*, 2013, **42**, 622–661.

34 J. Sun and X. He, AIE-based drug/gene delivery system: Evolution from fluorescence monitoring alone to augmented therapeutics, *Aggregate*, 2022, **3**, e282.

35 J.-T. Hou, W. X. Ren, K. Li, J. Seo, A. Sharma, X.-Q. Yu and J. S. Kim, Fluorescent bioimaging of pH: from design to applications, *Chem. Soc. Rev.*, 2017, **46**, 2076–2090.

36 H. Xiao, P. Li and B. Tang, Recent progresses in fluorescent probes for detection of polarity, *Coord. Chem. Rev.*, 2021, **427**, 213582.

37 H. Tian Jr, A. C. Sedgwick, H.-H. Han, S. Sen, G.-R. Chen, Y. Zang, J. L. Sessler, T. D. James, J. Li and X.-P. He, Fluorescent probes for the imaging of lipid droplets in live cells, *Coord. Chem. Rev.*, 2021, **427**, 213577.

38 S. K. Bhunia, A. Saha, A. R. Maity, S. C. Ray and N. R. Jana, Carbon Nanoparticle-based Fluorescent Bioimaging Probes, *Sci. Rep.*, 2013, **3**, 1473.

39 W. Xu, Z. Zeng, J.-H. Jiang, Y.-T. Chang and L. Yuan, Discerning the Chemistry in Individual Organelles with Small-Molecule Fluorescent Probes, *Angew. Chem., Int. Ed.*, 2016, **55**, 13658–13699.

40 D. Barman, K. Narang, R. Parui, N. Zehra, M. N. Khatun, L. R. Adil and P. K. Iyer, Review on recent trends and

prospects in π-conjugated luminescent aggregates for biomedical applications, *Aggregate*, 2022, **3**, e172.
41 Y. Huang, W. Chen, J. Chung, J. Yin and J. Yoon, Recent progress in fluorescent probes for bacteria, *Chem. Soc. Rev.*, 2021, **50**, 7725–7744.
42 B.-B. Chen, M.-L. Liu, Y.-T. Gao, S. Chang, R.-C. Qian and D.-W. Li, Design and applications of carbon dots-based ratiometric fluorescent probes: A review, *Nano Res.*, 2023, **16**, 1064–1083.
43 X. Gao, C. Du, Z. Zhuang and W. Chen, Carbon quantum dot-based nanoprobes for metal ion detection, *J. Mater. Chem. C*, 2016, **4**, 6927–6945.
44 X. Li, S. Zhao, B. Li, K. Yang, M. Lan and L. Zeng, Advances and perspectives in carbon dot-based fluorescent probes: Mechanism, and application, *Coord. Chem. Rev.*, 2021, **431**, 213686.
45 W. Chen, X. Ma, H. Chen, S. Hua Liu and J. Yin, Fluorescent probes for pH and alkali metal ions, *Coord. Chem. Rev.*, 2021, **427**, 213584.
46 T. Ha and P. Tinnefeld, Photophysics of Fluorescent Probes for Single-Molecule Biophysics and Super-Resolution Imaging, *Annu. Rev. Phys. Chem.*, 2012, **63**, 595–617.
47 J. Yin, L. Huang, L. Wu, J. Li, T. D. James and W. Lin, Small molecule based fluorescent chemosensors for imaging the microenvironment within specific cellular regions, *Chem. Soc. Rev.*, 2021, **50**, 12098–12150.
48 C. Wang, W. Chi, Q. Qiao, D. Tan, Z. Xu and X. Liu, Twisted intramolecular charge transfer (TICT) and twists beyond TICT: from mechanisms to rational designs of bright and sensitive fluorophores, *Chem. Soc. Rev.*, 2021, **50**, 12656–12678.
49 W. Sun, M. Li, J. Fan and X. Peng, Activity-Based Sensing and Theranostic Probes Based on Photoinduced Electron Transfer, *Acc. Chem. Res.*, 2019, **52**, 2818–2831.
50 H. Niu, J. Liu, H. M. O'Connor, T. Gunnlaugsson, T. D. James and H. Zhang, Photoinduced electron transfer (PeT) based fluorescent probes for cellular imaging and disease therapy, *Chem. Soc. Rev.*, 2023, **52**, 2322–2357.
51 X. Tian, L. C. Murfin, L. Wu, S. E. Lewis and T. D. James, Fluorescent small organic probes for biosensing, *Chem. Sci.*, 2021, **12**, 3406–3426.
52 H. S. Jung, P. Verwilst, W. Y. Kim and J. S. Kim, Fluorescent and colorimetric sensors for the detection of humidity or water content, *Chem. Soc. Rev.*, 2016, **45**, 1242–1256.
53 E. E. Jelley, Spectral Absorption and Fluorescence of Dyes in the Molecular State, *Nature*, 1936, **138**, 1009–1010.
54 J. L. Bricks, Y. L. Slominskii, I. D. Panas and A. P. Demchenko, Fluorescent J-aggregates of cyanine dyes: basic research and applications review, *Methods Appl. Fluoresc.*, 2017, **6**, 012001.
55 P. K. Misra and P. Somasundaran, in *Interfacial Processes and Molecular Aggregation of Surfactants*, ed. R. Narayanan, Springer Berlin Heidelberg, Berlin, Heidelberg, 2008, vol. 218, pp. 143–188.
56 A. Samanta, B. K. Paul and N. Guchhait, Modulation of Intramolecular Charge Transfer Emission Inside Micelles: A Fluorescence Probe for Studying Microenvironment of Micellar Assemblies, *J. Fluoresc.*, 2012, **22**, 289–301.
57 D. Qiao, L. Li, T. Shen, J. Yang, H. Chang, X. Liang, L. Zhang, Q. Wang, N. Liu, W. Zhao and L. Shang, Establishment of a Customizable Fluorescent Probe Platform for the Organelle-Targeted Bioactive Species Detection, *ACS Sens.*, 2020, **5**, 2247–2254.
58 G. Tian, Z. Zhang, H. Li, D. Li, X. Wang and C. Qin, Design, Synthesis and Application in Analytical Chemistry of Photo-Sensitive Probes Based on Coumarin, *Crit. Rev. Anal. Chem.*, 2021, **51**, 565–581.
59 H. Cao, Y. Xiong, T. Wang, B. Chen, T. C. Squier and M. U. Mayer, A red Cy3-based biarsenical fluorescent probe targeted to a complementary binding peptide, *J. Am. Chem. Soc.*, 2007, **129**, 8672–8673.
60 M. Sunbul and A. Jaeschke, Contact-Mediated Quenching for RNA Imaging in Bacteria with a Fluorophore-Binding Aptamer, *Angew. Chem., Int. Ed.*, 2013, **52**, 13401–13404.
61 S. Yoo and M. S. Han, A fluorescent probe for butyrylcholinesterase activity in human serum based on a fluorophore with specific binding affinity for human serum albumin, *Chem. Commun.*, 2019, **55**, 14574–14577.
62 Y.-D. Zhuang, P.-Y. Chiang, C.-W. Wang and K.-T. Tan, Environment-Sensitive Fluorescent Turn-On Probes Targeting Hydrophobic Ligand-Binding Domains for Selective Protein Detection, *Angew. Chem., Int. Ed.*, 2013, **52**, 8124–8128.
63 D. Monchaud, C. Allain and M.-P. Teulade-Fichou, Development of a fluorescent intercalator displacement assay (G4-FID) for establishing quadruplex-DNA affinity and selectivity of putative ligands, *Bioorg. Med. Chem. Lett.*, 2006, **16**, 4842–4845.
64 M. Oishi, S. Nakao and D. Kato, Enzyme-free fluorescent-amplified aptasensors based on target-responsive DNA strand displacement via toehold-mediated click chemical ligation, *Chem. Commun.*, 2014, **50**, 991–993.
65 Y. Zhang, X.-k. Du, X. Su, X. Zou and C.-Y. Zhang, Mismatched fluorescent probes with an enhanced strand displacement reaction rate for intracellular long noncoding RNA imaging, *Chem. Commun.*, 2022, **58**, 1760–1763.
66 J. J. Li, Y. Chu, B. Y.-H. Lee and X. S. Xie, Enzymatic signal amplification of molecular beacons for sensitive DNA detection, *Nucleic Acids Res.*, 2008, **36**, e36.
67 Y. K. Yang, K. J. Yook and J. Tae, A rhodamine-based fluorescent and colorimetric chemodosimeter for the rapid detection of Hg2+ ions in aqueous media, *J. Am. Chem. Soc.*, 2005, **127**, 16760–16761.
68 J. A. Carr, D. Franke, J. R. Caram, C. F. Perkinson, M. Saif, V. Askoxylakis, M. Datta, D. Fukumura, R. K. Jain, M. G. Bawendi and O. T. Bruns, Shortwave infrared fluorescence imaging with the clinically approved near-infrared dye indocyanine green, *Proc. Natl. Acad. Sci. U.S.A.*, 2018, **115**, 4465–4470.
69 H.-B. Cheng, Y. Li, B. Z. Tang and J. Yoon, Assembly strategies of organic-based imaging agents for

fluorescence and photoacoustic bioimaging applications, *Chem. Soc. Rev.*, 2020, **49**, 21–31.

70 Z. Hu, C. Fang, B. Li, Z. Zhang, C. Cao, M. Cai, S. Su, X. Sun, X. Shi, C. Li, T. Zhou, Y. Zhang, C. Chi, P. He, X. Xia, Y. Chen, S. S. Gambhir, Z. Cheng and J. Tian, First-in-human liver-tumour surgery guided by multispectral fluorescence imaging in the visible and near-infrared-I/II windows, *Nat. Biomed. Eng.*, 2020, **4**, 259–271.

71 W.-J. Guo, T. Peng, W. Zhu, S. Ma, G. Wang, Y. Li, B. Liu and H.-Q. Peng, Visualization of supramolecular assembly by aggregation-induced emission, *Aggregate*, 2023, **4**, e297.

72 X. Ye, Y. Liu, Y. Lv, G. Liu, X. Zheng, Q. Han, K. A. Jackson and X. Tao, In Situ Microscopic Observation of the Crystallization Process of Molecular Microparticles by Fluorescence Switching, *Angew. Chem., Int. Ed.*, 2015, **54**, 7976–7980.

73 X. Shi, J. Zhang, J. Liu, X. Zhao, H. Wang, P. Wei, X. Zhang, X.-L. Ni, H. H. Y. Sung, I. D. Williams, W. K. Ng, K. S. Wong, J. W. Y. Lam, L. Wang, H. Jin and B. Z. Tang, Hierarchical Supramolecular Self-assembly: Fabrication and Visualization of Multiblock Microstructures, *Angew. Chem., Int. Ed.*, 2022, **61**, e202211298.

74 T. Faisal, K. M. Solntsev, T. Kahs, N. i. Saleh, P. Commins, J. Whelan, S. Mohamed and P. Naumov, Formation of Noncovalent Complexes between Complex Mixtures of Polycyclic Aromatic Hydrocarbons (Asphaltenes) and Substituted Aromatics Studied by Fluorescence Spectroscopy, *Energy Fuels*, 2021, **35**, 8742–8755.

75 P. Chaudhuri, A. K. Ghosh and S. S. Panja, Study of Molecular Complex Formation of Coal-Derived Asphaltene with TCNQ in Homogeneous and Heterogeneous Media by UV-Vis and Fluorescence Spectroscopic Studies, *J. Dispersion Sci. Technol.*, 2016, **37**, 205–212.

76 A. K. Ghosh, P. Chaudhuri and S. S. Panja, Steady state fluorescence spectroscopic studies on the aggregation of coal derived asphaltene at lower concentration, *Fuel*, 2016, **185**, 164–170.

77 Y. Zhang, Applications of Noncontact Atomic Force Microscopy in Petroleum Characterization: Opportunities and Challenges, *Energy Fuels*, 2021, **35**, 14422–14444.

78 A. K. Ghosh, P. Chaudhuri, B. Kumar and S. S. Panja, Review on aggregation of asphaltene vis-a-vis spectroscopic studies, *Fuel*, 2016, **185**, 541–554.

79 S. Li, J. Opdam, L. G. J van der Ven, R. Tuinier and A. Catarina C Esteves, What is the role of PEO chains in the assembly of core-corona supraparticles in aqueous dispersions?, *J. Colloid Interface Sci.*, 2023, **646**, 461–471.

80 Y. Shen, H. Lin, M. Yang, X. Gong, B. Guan, Y. Han, S. Wang and Y. Wang, Hierarchical Superstructure of Plant Polyphenol and Arginine Surfactant for Long-Lasting and Target-Selective Antimicrobial Application, *Adv. Mater.*, 2023, **35**, 2210936.

81 G. N. Smith, P. Brown, S. E. Rogers and J. Eastoe, Evidence for a Critical Micelle Concentration of Surfactants in Hydrocarbon Solvents, *Langmuir*, 2013, **29**, 3252–3258.

82 A. P. Zhu, S. Dai, L. Li and F. Zhao, Salt effects on aggregation of O-carboxymethylchitosan in aqueous solution, *Colloids Surf., B*, 2006, **47**, 20–28.

83 N. A. B. Vieira, M. S. Moscardini, V. A. D. Tiera and M. J. Tiera, Aggregation behavior of hydrophobically modified dextran in aqueous solution: a fluorescence probe study, *Carbohydr. Polym.*, 2003, **53**, 137–143.

84 L. Zhao, Y. Yan and J.-B. Huang, Application of Fluorescent Probe Technology in Self-Assembly Systems of Amphiphile Aqueous Solutions, *Wuli Huaxue Xuebao*, 2010, **26**, 840–849.

85 P. Bharmoria, J. Vaneet, P. K. Banipal, A. Kumar and T. S. Kang, Modulation of Micellization Behavior of Cetyltrimethylammonium Bromide (CTAB) by Organic Anions in Low Concentration Regime, *J. Solution Chem.*, 2015, **44**, 16–33.

86 Q. Zhu, L. Huang, J. Su and S. Liu, A sensitive and visible fluorescence-turn-on probe for the CMC determination of ionic surfactants, *Chem. Commun.*, 2014, **50**, 1107–1109.

87 M. Megyesi and L. Biczok, Berberine alkaloid as a sensitive fluorescent probe for bile salt aggregates, *J. Phys. Chem. B*, 2007, **111**, 5635–5639.

88 L. Cognet, C. Tardin, M.-L. M. Negrier, C. Breillat, F. Coussen, D. Choquet and B. Lounis, Robust single-molecule approach for counting autofluorescent proteins, *J. Biomed. Opt.*, 2008, **13**, 031216.

89 J. A. Molina-Bolivar, J. M. Hierrezuelo and C. C. Ruiz, Self-assembly, hydration, and structures in N-decanoyl-N-methylglucamide aqueous solutions: Effect of salt addition and temperature, *J. Colloid Interface Sci.*, 2007, **313**, 656–664.

90 Y. Mylonas, G. Staikos and P. Lianos, Investigation of the poly(N-isopropylacrylamide) sodium dodecyl sulfate complexation with viscosity, dialysis, and time-resolved fluorescence-quenching measurements, *Langmuir*, 1999, **15**, 7172–7175.

91 M. Pisarcik, M. Polakovicova, M. Markuliak, M. Lukac and F. Devinsky, Self-Assembly Properties of Cationic Gemini Surfactants with Biodegradable Groups in the Spacer, *Molecules*, 2019, **24**, 1481.

92 Y. L. Jin, L. L. Ritcey, R. A. Speers and P. J. Dolphin, Effect of cell surface hydrophobicity, charge, and zymolectin density on the flocculation of Saccharomyces cerevisiae, *J. Am. Soc. Brew. Chem.*, 2001, **59**, 1–9.

93 R. Kraayenhof, G. J. Sterk, H. W. Wong Fong Sang, K. Krab and R. M. Epand, Monovalent cations differentially affect membrane surface properties and membrane curvature, as revealed by fluorescent probes and dynamic light scattering, *Biochim. Biophys. Acta*, 1996, **1282**, 293–302.

94 L. Jiang, M. Deng, Y. Wang, D. Liang, Y. Yan and J. Huang, Special Effect of beta-Cyclodextrin on the Aggregation Behavior of Mixed Cationic/Anionic Surfactant Systems, *J. Phys. Chem. B*, 2009, **113**, 7498–7504.

95 P. Sarkar and A. Chattopadhyay, Membrane Dipole Potential: An Emerging Approach to Explore Membrane Organization and Function, *J. Phys. Chem. B*, 2022, **126**, 4415–4430.

96 S. Haldar, R. K. Kanaparthi, A. Samanta and A. Chattopadhyay, Differential Effect of Cholesterol and Its Biosynthetic Precursors on Membrane Dipole Potential, *Biophys. J.*, 2012, **102**, 1561–1569.
97 X. Zheng, D. Wang, W. Xu, S. Cao, Q. Peng and B. Z. Tang, Charge control of fluorescent probes to selectively target the cell membrane or mitochondria: theoretical prediction and experimental validation, *Mater. Horiz.*, 2019, **6**, 2016–2023.
98 E. Gross, R. S. Bedlack and L. M. Loew, Dual-wavelength ratiometric fluorescence measurement of the membrane dipole potential, *Biophys. J.*, 1994, **67**, 208–216.
99 D. Maclaurin, V. Venkatachalam, H. Lee and A. E. Cohen, Mechanism of voltage-sensitive fluorescence in a microbial rhodopsin, *Proc. Natl. Acad. Sci. U.S.A.*, 2013, **110**, 5939–5944.
100 G. Yu, X. Yan, C. Han and F. Huang, Characterization of supramolecular gels, *Chem. Soc. Rev.*, 2013, **42**, 6697–6722.
101 I. R. Butler, D. M. Evans, P. N. Horton, S. J. Coles, S. F. Parker and S. C. Capelli, The spontaneous self-assembly of a molecular water pipe in 3D space, *Iucrj*, 2022, **9**, 364–369.
102 P. Xing, Y. Li, Y. Wang, P.-Z. Li, H. Chen, S. Z. F. Phua and Y. Zhao, Water-Binding-Mediated Gelation/Crystallization and Thermosensitive Superchirality, *Angew. Chem., Int. Ed.*, 2018, **57**, 7774–7779.
103 A. Vidyasagar and K. M. Sureshan, Stoichiometric Sensing to Opt between Gelation and Crystallization, *Angew. Chem., Int. Ed.*, 2015, **54**, 12078–12082.
104 N. Q. Hoffer and M. T. Woodside, Probing microscopic conformational dynamics in folding reactions by measuring transition paths, *Curr. Opin. Chem. Biol.*, 2019, **53**, 68–74.
105 C. A. Royer, Probing protein folding and conformational transitions with fluorescence, *Chem. Rev.*, 2006, **106**, 1769–1784.
106 X. Zhang, S. Rehm, M. M. Safont-Sempere and F. Würthner, Vesicular perylene dye nanocapsules as supramolecular fluorescent pH sensor systems, *Nat. Chem.*, 2009, **1**, 623–629.
107 M. F. Czar and R. A. Jockusch, Sensitive probes of protein structure and dynamics in well-controlled environments: combining mass spectrometry with fluorescence spectroscopy, *Curr. Opin. Struct. Biol.*, 2015, **34**, 123–134.
108 P. Tiwari, R. Wu, J. B. Metternich and R. Zenobi, Transition Metal Ion FRET in the Gas Phase: A 10-40 A Range Molecular Ruler for Mass-Selected Biomolecular Ions, *J. Am. Chem. Soc.*, 2021, **143**, 11291–11295.
109 K. Wang, Z. Tang, C. J. Yang, Y. Kim, X. Fang, W. Li, Y. Wu, C. D. Medley, Z. Cao, J. Li, P. Colon, H. Lin and W. Tan, Molecular Engineering of DNA: Molecular Beacons, *Angew. Chem., Int. Ed.*, 2009, **48**, 856–870.
110 S. Tyagi and F. R. Kramer, Molecular beacons: probes that fluoresce upon hybridization, *Nat. Biotechnol.*, 1996, **14**, 303–308.
111 A. C. Mendes, E. T. Baran, R. L. Reis and H. S. Azevedo, Self-assembly in nature: using the principles of nature to create complex nanobiomaterials, *Wiley Interdiscip. Rev.: Nanomed. Nanobiotechnology.*, 2013, **5**, 582–612.
112 N. E. Hernández, W. A. Hansen, D. Zhu, M. E. Shea, M. Khalid, V. Manichev, M. Putnins, M. Chen, A. G. Dodge, L. Yang, I. Marrero-Berríos, M. Banal, P. Rechani, T. Gustafsson, L. C. Feldman, S. H. Lee, L. P. Wackett, W. Dai and S. D. Khare, Stimulus-responsive self-assembly of protein-based fractals by computational design, *Nat. Chem.*, 2019, **11**, 605–614.
113 Y. Zhou, Q. Li, Y. Wu, X. Li, Y. Zhou, Z. Wang, H. Liang, F. Ding, S. Hong, N. F. Steinmetz and H. Cai, Molecularly Stimuli-Responsive Self-Assembled Peptide Nanoparticles for Targeted Imaging and Therapy, *ACS Nano*, 2023, **17**, 8004–8025.
114 H. Jin, Y. Zhou, W. Huang and D. Yan, Polymerization-like Multilevel Hierarchical Self-Assembly of Polymer Vesicles into Macroscopic Superstructures with Controlled Complexity, *Langmuir*, 2010, **26**, 14512–14519.
115 J. Zhuang, M. R. Gordon, J. Ventura, L. Li and S. Thayumanavan, Multi-stimuli responsive macromolecules and their assemblies, *Chem. Soc. Rev.*, 2013, **42**, 7421–7435.
116 A. Revil, C. D. Meyer and Q. Niu, A laboratory investigation of the thermoelectric effect, *Geophysics*, 2016, **81**, E243–E257.
117 A. Sarua, H. F. Ji, M. Kuball, M. J. Uren, T. Martin, K. P. Hilton and R. S. Balmer, Integrated micro-Raman/Infrared thermography probe for monitoring of self-heating in AlGaN/GaN transistor structures, *IEEE Trans. Electron Devices*, 2006, **53**, 2438–2447.
118 S. Wang, J. Jiang, Y. Lu, J. Liu, X. Han, D. Zhao and C. Li, Ratiometric fluorescence temperature sensing based on single- and dual-lanthanide metal-organic frameworks, *J. Lumin.*, 2020, **226**, 117418.
119 L. Marciniak, A. Bednarkiewicz, D. Kowalska and W. Strek, A new generation of highly sensitive luminescent thermometers operating in the optical window of biological tissues, *J. Mater. Chem. C*, 2016, **4**, 5559–5563.
120 J. F. Lou, T. M. Finegan, P. Mohsen, T. A. Hatton and P. E. Laibinis, Fluorescence-based thermometry: Principles and applications, *Rev. Anal. Chem.*, 1999, **18**, 235–284.
121 S. Arai, S.-C. Lee, D. Zhai, M. Suzuki and Y. T. Chang, A Molecular Fluorescent Probe for Targeted Visualization of Temperature at the Endoplasmic Reticulum, *Sci. Rep.*, 2014, **4**, 6701.
122 S. Ebrahimi, Y. Akhlaghi, M. Kompany-Zareh and A. Rinnan, Nucleic Acid Based Fluorescent Nanothermometers, *ACS Nano*, 2014, **8**, 10372–10382.
123 J. Qiao, C. Chen, L. Qi, M. Liu, P. Dong, Q. Jiang, X. Yang, X. Mu and L. Mao, Intracellular temperature sensing by a ratiometric fluorescent polymer thermometer, *J. Mater. Chem. B*, 2014, **2**, 7544–7550.
124 H. Wang, Y. Q. Wu, Y. L. Shi, P. Tao, X. Fan, X. Y. Su and G. C. Kuang, BODIPY-Based Fluorescent Thermometer as a Lysosome-Targetable Probe: How the Oligo(ethylene

glycols) Compete Photoinduced Electron Transfer, *Chem.–Eur. J.*, 2015, **21**, 3219–3223.

125 H. Wang, Y. Q. Wu, P. Tao, X. Fan and G. C. Kuang, BODIPY-Based Oligo(ethylene glycol) Dendrons as Fluorescence Thermometers: When Thermoresponsiveness Meets Intramolecular Electron/Charge Transfer, *Chem.–Eur. J.*, 2014, **20**, 16634–16643.

126 Y. Zheng, Y. Meana, M. M. A. Mazza, J. D. Baker, P. J. Minnett and F. M. Raymo, Fluorescence Switching for Temperature Sensing in Water, *J. Am. Chem. Soc.*, 2022, **144**, 4759–4763.

127 P. Wu, X. Hou, J.-J. Xu and H.-Y. Chen, Ratiometric fluorescence, electrochemiluminescence, and photoelectrochemical chemo/biosensing based on semiconductor quantum dots, *Nanoscale*, 2016, **8**, 8427–8442.

128 M. H. Lee, N. Park, C. Yi, J. H. Han, J. H. Hong, K. P. Kim, D. H. Kang, J. L. Sessler, C. Kang and J. S. Kim, Mitochondria-Immobilized pH-Sensitive Off-On Fluorescent Probe, *J. Am. Chem. Soc.*, 2014, **136**, 14136–14142.

129 S. Chakraborty, M. M. Joseph, S. Varughese, S. Ghosh, K. K. Maiti, A. Samanta and A. Ajayaghosh, A new pentacyclic pyrylium fluorescent probe that responds to pH imbalance during apoptosis, *Chem. Sci.*, 2020, **11**, 12695–12700.

130 A. M. Dennis, W. J. Rhee, D. Sotto, S. N. Dublin and G. Bao, Quantum Dot-Fluorescent Protein FRET Probes for Sensing Intracellular pH, *ACS Nano*, 2012, **6**, 2917–2924.

131 A. Liu, X. Huang, W. He, F. Xue, Y. Yang, J. Liu, L. Chen, L. Yuan and P. Xu, pHmScarlet is a pH-sensitive red fluorescent protein to monitor exocytosis docking and fusion steps, *Nat. Commun.*, 2021, **12**, 1413.

132 Z.-Y. Li, X.-L. Cui, M.-M. Xiao, J.-Y. Miao, B.-X. Zhao and Z.-M. Lin, An FRET-ICT-based ratiometric fluorescent and colorimetric probe for pH monitoring in lysosomes and water, *Dyes Pigm.*, 2021, **193**, 109481.

133 F. M. Jradi and L. D. Lavis, Chemistry of Photosensitive Fluorophores for Single-Molecule Localization Microscopy, *ACS Chem. Biol.*, 2019, **14**, 1077–1090.

134 D. Maurel, S. Banala, T. Laroche and K. Johnsson, Photoactivatable and Photoconvertible Fluorescent Probes for Protein Labeling, *ACS Chem. Biol.*, 2010, **5**, 507–516.

135 Z. Zou, Z. Luo, X. Xu, S. Yang, Z. Qing, J. Liu and R. Yang, Photoactivatable fluorescent probes for spatiotemporal-controlled biosensing and imaging, *Trends Anal. Chem.*, 2020, **125**, 115811.

136 J. Zhao, H. Chu, Y. Zhao, Y. Lu and L. Li, A NIR Light Gated DNA Nanodevice for Spatiotemporally Controlled Imaging of MicroRNA in Cells and Animals, *J. Am. Chem. Soc.*, 2019, **141**, 7056–7062.

137 J. V. Jun, C. M. Haney, R. J. Karpowicz Jr, S. Giannakoulias, V. M. Y. Lee, E. J. Petersson and D. M. Chenoweth, A "Clickable" Photoconvertible Small Fluorescent Molecule as a Minimalist Probe for Tracking Individual Biomolecule Complexes, *J. Am. Chem. Soc.*, 2019, **141**, 1893–1897.

138 D. Lee, C. Qian, H. Wang, L. Li, K. Miao, J. Du, D. M. Shcherbakova, V. V. Verkhusha, L. V. Wang and L. Wei, Toward photoswitchable electronic pre-resonance stimulated Raman probes, *J. Chem. Phys.*, 2021, **154**, 135102.

139 S. Spange, R. Sens, Y. Zimmermann, A. Seifert, I. Roth, S. Anders and K. Hofmann, A solvatochromic dye for probing significantly the dipolarity/polarizability of HBD (hydrogen bond donating) environments, *New J. Chem.*, 2003, **27**, 520–524.

140 A. S. Klymchenko, Solvatochromic and Fluorogenic Dyes as Environment-Sensitive Probes: Design and Biological Applications, *Acc. Chem. Res.*, 2017, **50**, 366–375.

141 O. A. Kucherak, P. Didier, Y. Mély and A. S. Klymchenko, Fluorene Analogues of Prodan with Superior Fluorescence Brightness and Solvatochromism, *J. Phys. Chem. Lett.*, 2010, **1**, 616–620.

142 B. Saremi, V. Bandi, S. Kazemi, Y. Hong, F. D'Souza and B. Yuan, Exploring NIR Aza-BODIPY-Based Polarity Sensitive Probes with ON-and-OFF Fluorescence Switching in Pluronic Nanoparticles, *Polymers*, 2020, **12**, 540.

143 B. Szczupak, A. G. Ryder, D. M. Togashi, A. S. Klymchenko, Y. A. Rochev, A. Gorelov and T. J. Glynn, Polarity Assessment of Thermoresponsive Poly(NIPAM-co-NtBA) Copolymer Films Using Fluorescence Methods, *J. Fluoresc.*, 2010, **20**, 719–731.

144 A. C. Sedgwick, L. Wu, H. H. Han, S. D. Bull, X. P. He, T. D. James, J. L. Sessler, B. Z. Tang, H. Tian and J. Yoon, Excited-state intramolecular proton-transfer (ESIPT) based fluorescence sensors and imaging agents, *Chem. Soc. Rev.*, 2018, **47**, 8842–8880.

145 S. Sasaki, G. P. C. Drummen and G.-i. Konishi, Recent advances in twisted intramolecular charge transfer (TICT) fluorescence and related phenomena in materials chemistry, *J. Mater. Chem. C*, 2016, **4**, 2731–2743.

146 K. Song and Z. Zhou, Two touching/self-assembly droplets in uniform Stokes flow: Viscous energy dissipation of the flow in droplets, *Phys. Fluids*, 2019, **31**, 012002.

147 D. L. Piet, A. V. Straube, A. Snezhko and I. S. Aranson, Viscosity Control of the Dynamic Self-Assembly in Ferromagnetic Suspensions, *Phys. Rev. Lett.*, 2013, **110**, 198001.

148 S. Moon, H. Kim, D. Kim and J. B. Lee, Viscosity-Regulated Control of RNA Microstructure Fabrication, *Polymers*, 2021, **13**, 454.

149 J. Sabin, J. M. Ruso, A. Gonzalez-Perez, G. Prieto and F. Sarmiento, Characterization of phospholipid plus semifluorinated alkane vesicle system, *Colloids Surf., B*, 2006, **47**, 64–70.

150 M. H. Gehlen and F. C. d. Schryver, Time-resolved fluorescence quenching in micellar assemblies, *Chem. Rev.*, 1993, **93**, 199–221.

151 A. Zheng, H. Liu, X. Gao, K. Xu and B. Tang, A Mitochondrial-Targeting Near-Infrared Fluorescent Probe for Revealing the Effects of Hydrogen Peroxide And Heavy Metal Ions on Viscosity, *Anal. Chem.*, 2021, **93**, 9244–9249.

152 Y. Song, H. Zhang, X. Wang, X. Geng, Y. Sun, J. Liu and Z. Li, One Stone, Three Birds: pH Triggered Transformation of Aminopyronine and Iminopyronine Based Lysosome Targeting Viscosity Probe for Cancer Visualization, *Anal. Chem.*, 2021, **93**, 1786–1791.

153 J. Zou, H. Lu, X. Zhao, W. Li, Y. Guan, Y. Zheng, L. Zhang and H. Gao, A multi-functional fluorescent probe with aggregation-induced emission characteristics: Mitochondrial imaging, photodynamic therapy and visualizing therapeutic process in zebrafish model, *Dyes Pigm.*, 2018, **151**, 45–53.

154 J. Yang, Y. Guo, M. Pistolozzi and J. Yan, Research progress of multi-functional fluorescent probes for Alzheimer's disease monitoring, *Dyes Pigm.*, 2021, **193**, 109466.

155 L. Zeng, G. Ma, J. Lin and P. Huang, Photoacoustic Probes for Molecular Detection: Recent Advances and Perspectives, *Small*, 2018, **14**, e1800782.

156 E. Y. Zhou, H. J. Knox, C. Liu, W. Zhao and J. Chan, A Conformationally Restricted Aza-BODIPY Platform for Stimulus-Responsive Probes with Enhanced Photoacoustic Properties, *J. Am. Chem. Soc.*, 2019, **141**, 17601–17609.

157 L. Yao, Y. Chen, J. Teng, W. Zheng, J. Wu, S. B. Adeloju, D. Pan and W. Chen, Integrated platform with magnetic purification and rolling circular amplification for sensitive fluorescent detection of ochratoxin A, *Biosens. Bioelectron.*, 2015, **74**, 534–538.

158 J. D. Slocum and L. J. Webb, Nitrile Probes of Electric Field Agree with Independently Measured Fields in Green Fluorescent Protein Even in the Presence of Hydrogen Bonding, *J. Am. Chem. Soc.*, 2016, **138**, 6561–6570.

159 I. T. Suydam and S. G. Boxer, Vibrational Stark Effects Calibrate the Sensitivity of Vibrational Probes for Electric Fields in Proteins, *Biochemistry*, 2003, **42**, 12050–12055.

160 S. S. Andrews and S. G. Boxer, Vibrational Stark Effects of Nitriles I. Methods and Experimental Results, *J. Phys. Chem. A*, 2000, **104**, 11853–11863.

161 Z. Li, K. Xiao, Q. Wan, R. Tang, K.-H. Low, X. Cui and C.-M. Che, Controlled Self-assembly of Gold(I) Complexes by Multiple Kinetic Aggregation States with Nonlinear Optical and Waveguide Properties, *Angew. Chem., Int. Ed.*, 2023, **62**, e202216523.

162 J. Seo, M. I. Khazi, K. Bae and J.-M. Kim, Temperature-Controlled Pathway Complexity in Self-Assembly of Perylene Diimide-Polydiacetylene Supramolecule, *Small*, 2023, **19**, 2206428.

163 N. D. Younan and J. H. Viles, A Comparison of Three Fluorophores for the Detection of Amyloid Fibers and Prefibrillar Oligomeric Assemblies. ThT (Thioflavin T); ANS (1-Anilinonaphthalene-8-sulfonic Acid); and bisANS (4,4'-Dianilino-1,1 '-binaphthyl-5,5 '-disulfonic Acid), *Biochemistry*, 2015, **54**, 4297–4306.

164 C.-B. Huang, L. Xu, J.-L. Zhu, Y.-X. Wang, B. Sun, X. Li and H.-B. Yang, Real-Time Monitoring the Dynamics of Coordination-Driven Self-Assembly by Fluorescence-Resonance Energy Transfer, *J. Am. Chem. Soc.*, 2017, **139**, 9459–9462.

165 P.-P. Jia, L. Xu, Y.-X. Hu, W.-J. Li, X.-Q. Wang, Q.-H. Ling, X. Shi, G.-Q. Yin, X. Li, H. Sun, Y. Jiang and H.-B. Yang, Orthogonal Self-Assembly of a Two-Step Fluorescence-Resonance Energy Transfer System with Improved Photosensitization Efficiency and Photooxidation Activity, *J. Am. Chem. Soc.*, 2021, **143**, 399–408.

166 B. Shi, P. Qin, W. Li, H. Feng, Y. Zhou, Y. Chai, W.-J. Qu, T.-B. Wei, Y.-M. Zhang and Q. Lin, A Two-Step Fluorescence-Resonance Energy Transfer System Constructed by Platinum(II) Metallacycle Based Molecular Recognition, *Inorg. Chem.*, 2023, **62**, 17236–17240.

167 Z. Wu, H. Qian, X. Li, T. Xiao and L. Wang, Recent advances in two-step energy transfer light-harvesting systems driven by non-covalent self-assembly, *Chin. Chem. Lett.*, 2024, **35**, 108829.

168 H. M. Watrob, C.-P. Pan and M. D. Barkley, Two-Step FRET as a Structural Tool, *J. Am. Chem. Soc.*, 2003, **125**, 7336–7343.

169 Y. Zhang, C. Yan, C. Wang, Z. Guo, X. Liu and W.-H. Zhu, A Sequential Dual-Lock Strategy for Photoactivatable Chemiluminescent Probes Enabling Bright Duplex Optical Imaging, *Angew. Chem., Int. Ed.*, 2020, **59**, 9059–9066.

170 Y. Fan, Y. Wu, J. Hou, P. Wang, X. Peng and G. Ge, Coumarin-based near-infrared fluorogenic probes: Recent advances, challenges and future perspectives, *Coord. Chem. Rev.*, 2023, **480**, 215020.

171 A. B. Isaev, N. S. Shabanov, A. G. Magomedova, P. V. Nidheesh and M. A. Oturan, Electrochemical oxidation of azo dyes in water: a review, *Environ. Chem. Lett.*, 2023, **21**, 2863–2911.

172 A. Ayati, M. N. Shahrak, B. Tanhaei and M. Sillanpää, Emerging adsorptive removal of azo dye by metal–organic frameworks, *Chemosphere*, 2016, **160**, 30–44.

173 S. Zafar, D. A. Bukhari and A. Rehman, Azo dyes degradation by microorganisms – An efficient and sustainable approach, *Saudi J. Biol. Sci.*, 2022, **29**, 103437.